Covert Localization in Wireless Networks: Feasibility and Performance Analysis

Yue Zhao, *Graduate Student Member, IEEE*, Zan Li, *Senior Member, IEEE*, Nan Cheng, *Member, IEEE*, Wei Wang, *Member, IEEE*, Chenxi Li, *Graduate Student Member, IEEE*, and Xuemin Shen, *Fellow, IEEE*

Abstract—In this paper, we propose covert localization to improve the security of wireless localization networks, which can prevent the legitimate transmission of localization signals between anchors and agent from being detected by the illegitimate warden. Specifically, we first establish a framework of covert localization and demonstrate its feasibility when the warden suffers noise uncertainty. Then, with two specific noise uncertainty distributions, we derive the fundamental limit of localization accuracy, i.e., covert squared position error bound (CSPEB), which is the achievable localization accuracy for the agent while ensuring covertness for the warden. Theoretical analysis of CSPEB demonstrates the impact of different factors on the localization accuracy. Besides, in an energy-constrained scenario, we formulate a power allocation problem to refine anchors' power to minimize the CSPEB for a given total power budget and develop an algorithm based on the semidefinite program (SDP). Simulation results verify our theoretical analysis by evaluating the effect of several representative factors on the CSPEB and show the superiority of the SDP-based power allocation algorithm to the other baseline methods.

Index Terms—Physical layer security, covert localization, noise uncertainty distributions, low probability of detection, covert squared position error bound (CSPEB).

I. INTRODUCTION

A. Background and Motivation

HIGH precision localization is the prerequisite for numerous location-based wireless services and applications,

such as Intelligent Transportation Systems (ITSs), Internet of Things (IoTs), and many military activities [1]–[6]. Plenty of research efforts have been dedicated to improving the localization accuracy, presuming reliable localization systems in the absence of adversarial eavesdroppers [7]–[10]. Nevertheless, one potential issue is that the malicious warden may attack the legitimate localization system by spoofing the agent and attacking the anchor network [11], in which anchors provide localization signals to assist the agent estimating its position. In some cases, identifying and preventing illegitimate attacks is not sufficient for the localization network. It is required to locate covertly by *covert localization* technique, which completes the localization process and prevents the transmitted signals of the anchor network from being detected by the warden. Covert localization is part of the physical layer security and has a significant impact on personal and public security. From the civil perspective, the agent can complete the localization process covertly to escape from the adversary's monitoring or tracking and to perform a secure position act. For some military operations, the disclosure of the localization process may lead to devastating attacks on the entire localization system [11]–[13]. Therefore, catering to such security concerns motivates the interest in covert localization.

There are two typical applications of covert localization and technique: 1) external location spoofing [8], [11], [14]; and 2) location privacy protection [11]–[13]. In the first scenario, an external attacker modifies the observations of the agent and then deteriorates the agent's localization accuracy. The hostile attacker would attack the localization system by operating localization signals, such as jamming, delaying, and modifying the power level [11]. The basic premise, in this case, is that the transmitted signals of anchors are detected and intercepted by the attacker. In the second scenario, wireless signals for communication or monitoring may be used by the eavesdropper to estimate the positions of network nodes and critical events, which results in the privacy disclosure of the entire network. Zhang *et al.* [13] proposed a location privacy protection approach based on power allocation, in which a passive eavesdropper estimated the position of the agent by intercepting the signal transmitted from the agent and round trip signals transmitted from the anchors. In this case, the eavesdropper cannot perceive the presence of transmission if the signal from the agent is not detected, and the eavesdropper cannot estimate the position

of the agent if the round trip signals from anchors are not detected.

It is of vital interest that the localization process stays covert from the illegitimate warden, which takes precedence over preventing the potential localization attacks. However, the feasibility conditions of covert localization are not clear. Meanwhile, there are no metrics to measure the performance of covert localization. Thus, to address many intending issues in covert localization, we aim to verify the feasibility from the perspective of signal detection and to provide an analytical framework for the covert localization accuracy. Our theoretical analysis provides useful insights into the design and operations of covert localization networks and is easily extended to other complicated scenarios.

B. Related Work

Nowadays, plenty of research efforts have been dedicated to studying parameter estimation and localization algorithms to improve the localization accuracy [11]. However, security in the localization system becomes of a more significant concern than ever because location-based information and system are now used for various vital applications and services [15]. In this section, literature related to secure localization is mentioned to review several existing techniques. Moreover, we introduce covert communication and try to leverage a similar principle to achieve covert localization.

1) Secure Localization: Location security is outlined in [15] as "protecting location information and systems from location security risks in order to ensure the quality of location security services". The purpose of the adversary in the localization network is to deteriorate the accuracy of the agent or to destroy the anchor network when the localization process occurs. There are two types of attackers in the localization system: (i) internal attackers, which report false localization information to cheat on their positions; and (ii) external attackers, which modify the parameter measurements [16]. For instance, the malicious or emissary anchor can be seen as an internal attacker, and the notorious location spoofing attacker can be regarded as an external attacker. The most straightforward manner for external attackers to achieve its goal is to intercept, jam, modify, and replay localization signals transmitted from anchors. Thus, the power level and the transmission delay of received signals for the agent are modified, and the position estimation is severely distorted [14], [16], [17].

Many strategies and manners are proposed coping with different types of potential threats and attackers. On one hand, if the localization attackers are detected and identified, compromised signals and data can be removed directly or be utilized to improve the localization accuracy by joint estimation [17]–[20]. Liu *et al.* [20] proposed a suite of methods to detect malicious nodes and to filter out replayed node signals. The basic idea for finding a malicious node was to compare the estimation position and its declared location, namely the geometric inconsistency [18], by using the signal interaction between the assistance node with known position and the malicious node. On the other hand, several attack-tolerant localization algorithms were proposed to compute the

agent's position robustly [21], such as robust statistical methods [22], voting-based estimation [17], and extra hardware-based scheme [23]. In particular, Li *et al.* [22] proposed a robust least median square (LMS)-based localization algorithm by minimizing the median of the residue squares to eliminate the effect of outliers caused by malicious attackers.

However, the main issue of the works mentioned above is that the attacker may know the existence of the transmission process and even intercept the signal of the anchor network. In contrast, the covert localization technique dedicates to operating the signal detection process of the adversary, such that attackers are unaware of the existence of the localization process.

2) Covert Communication: Covert communication focuses on hiding wireless transmission between the transmitter and the receiver, preventing the possibility of the warden attempting to detect communication signals [24]–[32]. Encryption-based security can prevent unauthorized decoding by the adversary and protect the content of the message [24]. In some instances, protecting the content of the transmitted information is insufficient [25], whereas covert communication is required to prevent the existence of transmission from being detected by the adversary [26].

A feasible approach to achieve positive-rate covert communication is exposing the illegitimate warden to uncertainties, e.g., channel fading uncertainty [24], interference uncertainty [26], and noise uncertainty [27], such that transmitted signals may be undetected by the warden. Noise uncertainty of the illegitimate warden should be considered and involved in a practical detection process because there are no perfect receiver devices and extremely accurate wireless communication channels in the real-world [28], [33]. Specifically, noise uncertainty can affect the signal detection of the warden by resulting in the SNR wall [33]. If the illegitimate warden is uncertain of surrounding noise level, undetectable communication between legitimate transmitter and receiver is possible when the transmit power is below a certain SNR level [34]. Based on the analysis of the SNR wall, Lee *et al.* [27] illustrated the realization of a positive error-free communication rate without being detected by an illegitimate warden. It may be the first work to study the undetectable communication with a positive rate. However, the detection performance of the warden in [27] was analyzed under the worst noise uncertainty. Furthermore, He *et al.* [28] introduced two distribution models to describe noise uncertainty, bounded and unbounded models, and investigated the covert transmission rate. Besides, Shahzad *et al.* [24] studied hiding the communication to a covert receiver by considering the fading uncertainty of warden and utilizing the transmission to another normal receiver as a cover. Hu *et al.* [29] considered the amplify-and-forward one-way relay network, where the relay opportunistically transmitted its information on top of forwarding the source's message, while the additional information needed to be covert for the source. In [29], the uncertainty was inherently embedded in the strategy for the relay to forward the original information of the source. Besides, as mentioned in [26], [28], [30], [31], interference signals or artificial noise can be emitted intentionally by the friendly jammer or the full-duplex receiver,

to increase the uncertainty for the warden and to provide the opportunity of achieving covert communication.

However, the above-mentioned papers of covert communication have not considered the covertness issues of signals in wireless localization networks. The lack of metrics to measure localization performance with covertness inspires us to investigate the feasibility and accuracy of covert localization.

C. Main Contributions

In this paper, we develop a theoretical framework to analyze the covert localization accuracy in range-based, i.e., time of arrival (TOA), wireless localization network, in which the anchor network transmits localization signals to help the legitimate agent estimate its position, while the existence of localization signals cannot be detected by an illegitimate warden. Covert localization can be achieved when the warden suffers noise uncertainty, i.e., the warden does not know the exact power of background noise [33] but only its value interval or distribution. We assume that the passive warden uses a primary and well-known energy detector, i.e., radiometer [34], to detect the presence of the legitimate signals, since energy detector can be used when little or no knowledge of the signal structure is available [35]. Based on the derivation of covert squared position error bound (CSPEB), we show that the accuracy of covert localization is affected by the noise uncertainty parameter, covertness requirement coefficient, the warden's position uncertainty, geometry of the network, and the nominal background noise. Furthermore, we formulate the power allocation optimization problem of the anchors in the presence of the total power constraint, and propose an algorithm based on the semidefinite program (SDP) to solve the problem. Simulation results validate our theoretical analysis by assessing the effect of the above-mentioned factors on the CSPEB. Moreover, simulations illustrate that the proposed SDP-based power allocation algorithm performs better than the other two baselines.

The main contributions are summarized as follows.

- We define a covert localization scenario, where a legitimate agent estimates its position by receiving the localization signals transmitted from the anchor network, while the transmission process is eavesdropped by an illegitimate warden that performs detection for the localization signals.
- We validate that the presence of noise uncertainty is beneficial for covert localization, and discuss the relationship between the warden's detection threshold and the experienced noise power to achieve covert localization.
- We analyze the optimal detection threshold for the warden when the noise uncertainty follows two different distributions, i.e., bounded uncertainty model (BUM) and unbounded uncertainty model (UUM). Furthermore, with both BUM and UUM, we derive the CSPEBs as the fundamental limits to measure covert localization accuracy when the warden holds the optimal thresholds. Besides, the worst-case CSPEB is derived in the presence of the illegitimate warden's position uncertainty. Theoretical
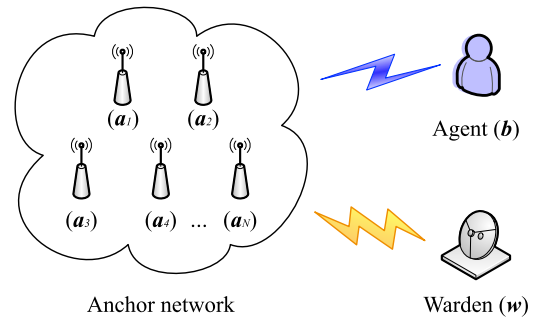
Fig. 1. Illustration of the wireless covert localization network.

analysis is provided to discuss the impact of different parameters on the CSPEB.

- We formulate a power allocation problem in the covert localization scenario to optimize the transmit powers of the anchors constraining the total available power. By utilizing the convexity of the Fisher information matrix to the anchors' power and considering the maximum power constraint of the anchors' signal not being detected, the nonconvex optimization problem can be transformed into a semidefinite program and then solved.

The remainder of this paper is organized as follows. Section II describes the system model. In Section III, we analyze the detection strategy for the illegitimate warden. Section IV provides localization accuracy metrics for the legitimate agent. Section V presents the theoretical analysis of covert localization with noise uncertainty distributions. Simulation results and discussions are given in Section VI. Finally, conclusions are drawn in Section VII.

Throughout the paper, we adopt the following notations. $\mathcal{N}(\cdot)$ and $\mathcal{Q}(\cdot)$ denote normal distribution and the tail probability of the standard normal distribution, respectively. $\text{erf}(\cdot)$ denotes the Gaussian error function and $\text{erf}^{-1}(\cdot)$ denotes the inverse error function. $\exp(\cdot)$ is the exponential function. $\mathbb{P}(\cdot)$ represents the probability.

II. SYSTEM MODEL

A. Network Setting

We consider a general 2-dimensional (2D) active localization scenario, where the anchor network transmits radio frequency (RF) localization signals covertly to a legitimate agent without being detected by an illegitimate warden. In the active localization scenario shown in Fig. 1, the agent determines its position by extracting the localization parameters from the received signals emitted from anchors with known positions. The anchor network consists of N anchors, and the set of anchors is denoted by $\mathcal{N}_a = \{1, 2, \cdots, N\}$. The warden, being passive, silently eavesdrops the transmission of the anchor network and tries to detect localization signals. Let $\boldsymbol{a}_i \in \mathcal{R}^2$ be the position of the ith anchor, while $\boldsymbol{b} \in \mathcal{R}^2$ and $\boldsymbol{w} \in \mathcal{R}^2$ represent the position of the agent and the warden, respectively. In this paper, we focus on the range-based localization system, where TOA is regarded as the localization parameter and the transmitter-receiver pair is synchronized. The distance between the anchor $\boldsymbol{a}_i$ and the

agent $\boldsymbol{b}$ can be expressed by the Euclidean norm,

$$d_{i,b} = \|\boldsymbol{a}_i - \boldsymbol{b}\|_2, \tag{1}$$

which can be easily converted to TOA by dividing the speed of radio signal c.

B. Transmission Signals

In general, localization signals are broadcast from the anchor network and are received by the agent and the warden over the complicated wireless channels. We assume that each transmitter or receiver equips a single antenna, and RF signal from each anchor propagates via a single line-of-sight (LOS) path with additive white Gaussian noise. This assumption may not necessarily be satisfied in practice, but obtained results will provide useful insights into the covert localization problem, and can be extended to more realistic environments, e.g., multipath propagation and complex fading.

For the agent, the received signal from anchor $\boldsymbol{a}_i$ can be written as [36], [37]

$$r_{i,b}(nT) = \sqrt{\frac{A^o P_i^t}{d_{i,b}^\varrho}} s(nT - \tau_{i,b}) + v_{i,b}(nT), \quad nT = T_{ob}, \tag{2}$$

where n is the sample index and T is the sample period. A^o is a proper constant to describe the wireless channel, T_{ob} is the observation period, $\tau_{i,b}$ is propagation delay, i.e., TOA, and ϱ indicates pathloss factor with $\varrho = 2$ in this paper. $s(nT)$ is a normalized waveform with unit energy and is transmitted by anchor $\boldsymbol{a}_i$ with power P_i^t. $v_{i,b}(nT)$ denotes the zero-mean Gaussian random noise with two-side power spectral density $N_0/2$. We assume that $s(nT)$ and $v_{i,b}(nT)$ are mutually independent.

Similarly, we assume that the warden has enough information to discriminate signals transmitted from different anchors. For instance, the warden can perform sensing for a specific frequency band in FDMA [13], where each anchor has a different frequency band and is known by the warden. Then, the received signal at the warden from anchor $\boldsymbol{a}_i$ can be given as

$$r_{i,w}(nT) = \sqrt{\frac{A^o P_i^t}{d_{i,w}^\varrho}} s(nT - \tau_{i,w}) + v_{i,w}(nT), \quad nT = T_{ob}, \tag{3}$$

where $\tau_{i,w}$ and $v_{i,w}$ are defined similarly to $\tau_{i,b}$ and $v_{i,b}$.

C. Noise Uncertainty Distributions

We consider a realistic scenario that the warden does not know its exact noise power, but only the noise uncertainty distributions. In this paper, two representative noise uncertainty distributions are used to analyze the accuracy of covert localization, one based on a uniform distribution called bounded uncertainty model (BUM), and the other based on a Gaussian distribution called unbounded uncertainty model (UUM) [28].

1) BUM: The exact noise power for the warden σ_w^2 follows a log-uniform distribution in an uncertainty interval Σ_I,

$$f_{\sigma_w^2}^{BUM}(x) = \begin{cases} \dfrac{1}{2\ln(\rho)x}, & x \in \Sigma_I, \\ 0, & \text{otherwise}, \end{cases} \tag{4}$$

where the noise uncertainty interval is $\Sigma_I = [\frac{1}{\rho}\sigma_n^2, \rho\sigma_n^2]$, σ_n^2 is the nominal noise power, and $\rho \geq 1$ is the parameter that quantifies the size of the noise uncertainty. Obviously, $\rho = 1$ means that the warden knows the exact noise power without uncertainty.

2) UUM: The noise power lies in an infinite range, i.e., $\sigma_w^2 \in [-\infty, \infty]$, and is related to a nominal noise power σ_n^2 through the following log-normal distribution

$$f_{\sigma_w^2}^{UUM}(x) = \begin{cases} \dfrac{\exp\left(-\dfrac{(\ln(x) - k\sigma_{n,\mathrm{dB}}^2)^2}{2k^2\sigma_{\Delta,\mathrm{dB}}^2}\right)}{x\sqrt{2\pi k^2\sigma_{\Delta,\mathrm{dB}}^2}}, & \text{if } x > 0, \\ 0, & \text{otherwise}, \end{cases} \tag{5}$$

where $k = \ln(10)/10$, $\sigma_{w,\mathrm{dB}}^2 = 10\log_{10}\sigma_w^2$, and $\sigma_{n,\mathrm{dB}}^2 = 10\log_{10}\sigma_n^2$. Note that, $\sigma_{\Delta,\mathrm{dB}}^2$ is the parameter to describe the noise uncertainty, and denotes the variance of the difference of $\sigma_{w,\mathrm{dB}}^2$ and $\sigma_{n,\mathrm{dB}}^2$ through a Gaussian distribution $(\sigma_{w,\mathrm{dB}}^2 - \sigma_{n,\mathrm{dB}}^2) \sim \mathcal{N}(0, \sigma_{\Delta,\mathrm{dB}}^2)$. With log-normal distribution, the expectation and variance of σ_w^2 are $\mu_1 = \exp(k\sigma_{n,\mathrm{dB}}^2 + k^2\sigma_{\Delta,\mathrm{dB}}^2/2)$ and $\mu_2 = (\exp(k^2\sigma_{\Delta,\mathrm{dB}}^2) - 1)\exp\left(2k\sigma_{n,\mathrm{dB}}^2 + k^2\sigma_{\Delta,\mathrm{dB}}^2\right)$, respectively.

D. Uncertainty of the Warden's Position

In addition to noise uncertainty distributions, the warden's position may also be uncertain for the legitimate localization system. The statistical distribution of the warden's position is not explored in this paper, but we consider the probable existence area of the warden. Specifically, we focus on the worst-case for the transmission strategy of anchors when the warden is in an uncertain area, and analyze the covert localization accuracy for the agent in this case. We assume that the position of the warden has the maximum uncertainty Δw, which is a positive scalar to describe the uncertain area. Namely, the warden is located within a circle $\mathscr{C}(\boldsymbol{w}, \Delta w)$, centered at the nominal position $\boldsymbol{w}$ with radius Δw. Thus, the distance between the warden and anchor $\boldsymbol{a}_i$ lies in the following set,

$$\tilde{d}_{i,w} = \|\boldsymbol{a}_i - \tilde{\boldsymbol{w}}\|_2 \in [d_{i,w} - \Delta w, d_{i,w} + \Delta w], \tag{6}$$

where $\tilde{\boldsymbol{w}}$ is the uncertain position of the warden, $d_{i,w}$ is the nominal distance between anchor $\boldsymbol{a}_i$ and the nominal position of the warden $\boldsymbol{w}$. Fig. 2 provides an example of the warden's position uncertainty model. For simplicity, we assume that the noise uncertainty distribution in the uncertain circle is constant.

III. DETECTION STRATEGY FOR THE WARDEN

In this section, we focus on the detection strategy for the warden to detect the existence of the localization signals transmitted from anchors. We first present the hypothesis testing that the warden confronts, and then discuss the
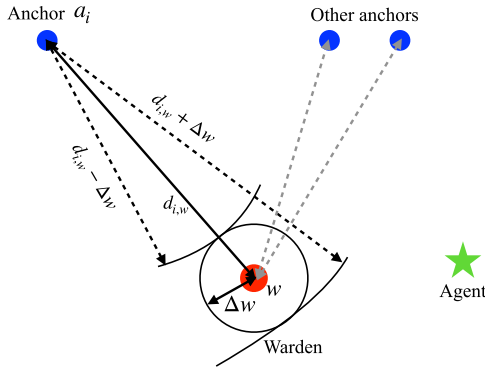
Fig. 2.   Geometric interpretation of the warden's position uncertainty.

realization of covert localization when the warden suffers noise uncertainty. Moreover, we introduce the definition of the average covert probability (ACP) to measure the covertness with noise uncertainty distributions. From the warden's perspective, we also derive the optimal detection threshold values to detect localization signals with both BUM and UUM distributions.

A. Hypothesis Testing

Considering the optimal circumstance for the passive warden, the signals transmitted from the anchors are separately detected by the warden based on the partial prior information, e.g., the frequency band and noise power. Here, the anchor a_i is used as an example to analyze the warden's detection performance. According to the passive observations within a period of time, the warden wishes to make a decision to discriminate between the null hypothesis ($\mathcal{H}_{i,0}$) and the alternative hypothesis ($\mathcal{H}_{i,1}$):

$$\mathcal{H}_{i,0} : r_{i,w}[n] = v_{i,w}[n], \tag{7}$$

$$\mathcal{H}_{i,1} : r_{i,w}[n] = \sqrt{\frac{A^o P_i^t}{d_{i,w}^\varrho}} s[n] + v_{i,w}[n], \tag{8}$$

where sample period T is omitted here. $\mathcal{H}_{i,0}$ denotes that localization signal is absent and $\mathcal{H}_{i,1}$ represents that the localization signal exists.

In this paper, the warden uses a radiometer as its detection testing [33], i.e.,

$$\mathcal{T}(r_{i,w}) = \frac{1}{N_s} \sum_{n=1}^{N_s} r_{i,w}[n] * r_{i,w}[n] \mathop{\gtrless}_{\mathcal{D}_{i,0}}^{\mathcal{D}_{i,1}} \gamma_i, \tag{9}$$

where N_s is the number of samples, γ_i is the predetermined detection threshold to detect the signal from anchor a_i, and two decisions $\mathcal{D}_{i,0}$ and $\mathcal{D}_{i,1}$ are to indicate the received signal of the warden: noise and localization signal plus noise, respectively.

Therefore, the false alarm probability and the misdetection probability for the warden can be defined as $\mathbb{P}_{i,FA} = \mathbb{P}(\mathcal{D}_{i,1}|\mathcal{H}_{i,0})$ and $\mathbb{P}_{i,MD} = \mathbb{P}(\mathcal{D}_{i,0}|\mathcal{H}_{i,1})$, respectively. Based on the central limit theorem and other approximations [27],

[28], [33], we have

$$\lim_{N_s \to \infty} \mathbb{P}_{i,FA} = \begin{cases} 0, & \text{if } \gamma_i > \sigma_w^2, \\ 1, & \text{if } \gamma_i < \sigma_w^2, \end{cases}$$

$$\lim_{N_s \to \infty} \mathbb{P}_{i,MD} = \begin{cases} 0, & \text{if } \gamma_i < P_{i,w}^r + \sigma_w^2, \\ 1, & \text{if } \gamma_i > P_{i,w}^r + \sigma_w^2. \end{cases} \tag{10}$$

where $N_s \to \infty$ means that the warden is allowed to observe an infinite number of samples [27], [28], σ_w^2 is the exact noise power at the warden, and $P_{i,w}^r = \frac{A^o P_i^t}{d_{i,w}^\varrho}$ is the power of received signal emitted from anchor a_i. Similar to existing studies on covert communication [25], [27], the error detection of the warden's hypothesis testing is measured by $\delta_i = \mathbb{P}_{i,FA} + \mathbb{P}_{i,MD}$, which satisfies

$$\delta_i = \begin{cases} 0, & \text{if } \sigma_w^2 < \gamma_i < P_{i,w}^r + \sigma_w^2, \\ 1, & \text{otherwise.} \end{cases} \tag{11}$$

Note that δ_i is also bounded between 0 and 1 [27]. $\delta_i = 0$ indicates that the warden can detect the transmission without error. In contrast, $\delta_i = 1$ indicates that the warden cannot detect the transmission at all.

B. Achieving Covert Localization With Noise Uncertainty

The goals of the legitimate agent, anchors, and the illegitimate warden are different. The warden wishes to minimize the probability of error detection $\delta_i = \mathbb{P}_{i,FA} + \mathbb{P}_{i,MD}$, for $\forall i \in \mathcal{N}_a$ and thus accurately senses the existence of the localization process. In contrast, the purpose of the anchors and the agent is to achieve covert localization, i.e., undetectable localization.

From the analysis of the warden's hypothesis testing, if the warden knows the exact noise power σ_w^2 without uncertainty and sets the detection threshold $\gamma_i \in (\sigma_w^2, P_{i,w}^r + \sigma_w^2)$, we have $\delta_i \to 0$ as $N_s \to \infty$, which implies that the warden can detect the transmission without any error when the observation time is infinite. Instead, the warden cannot perfectly detect the signal when the threshold and noise power satisfy [27]

$$\gamma_i < \sigma_w^2 \quad \text{or} \quad \gamma_i > P_{i,w}^r + \sigma_w^2. \tag{12}$$

Hence, noise uncertainty can be involved to coordinate the relationship between the detection threshold and received power. With noise uncertainty, the warden only knows that the noise power may be contained in a specific interval, instead of its exact value.

We use the noise uncertainty interval $\bar{\Sigma}_I = [\frac{1}{\rho}\sigma_n^2, \rho\sigma_n^2]$ as an example to illustrate the realization of covert localization. For a given $\bar{\Sigma}_I$, ρ has the same meaning as that of BUM, but the noise distribution is not considered here. If the upper limit of noise uncertainty is smaller than the lower limit of noise uncertainty plus received signal power, i.e., $\rho\sigma_n^2 < \frac{1}{\rho}\sigma_n^2 + P_{i,w}^r$, the warden can set the threshold between $\rho\sigma_n^2$ and $\frac{1}{\rho}\sigma_n^2 + P_{i,w}^r$, and can detect the signal transmitted from anchor a_i with $\delta_i \to 0$. In contrast, if the upper limit of noise uncertainty is greater than the lower limit of noise uncertainty plus received signal power, i.e., $\rho\sigma_n^2 > \frac{1}{\rho}\sigma_n^2 + P_{i,w}^r$, the warden may not detect the signal correctly without appropriate threshold and the signal transmitted from anchor a_i can be covert

for the warden. In other words, covert localization can be achieved when two power intervals, i.e., the noise uncertainty interval and the noise uncertainty plus signal interval, intersect. Therefore, with a noise uncertainty interval $\bar{\Sigma}_I$, $\rho - \frac{1}{\rho}$ is known as the SNR wall for signal detection [27], [33].

C. Covertness Measure

In the previous analysis, we demonstrate that the covert localization can be achieved when the warden suffers uncertain noise power. For a specific noise uncertainty distribution, assuming the warden utilizes the optimal thresholds to separately detect anchors' signals, the overall performance of covertness should be measured by the average covert probability [28], which captures the average covertness from a Bayesian statistics perspective [25].

Definition 1: The average covert probability (ACP) is

$$\bar{\delta}_i = \int_0^\infty \min_{\gamma_i} \delta_i(\sigma_w^2, \gamma_i) f_{\sigma_w^2}(\sigma_w^2) d\sigma_w^2, \qquad (13)$$

where $\min_{\gamma_i}$ denotes that the warden detects the localization signals by using the optimal detection thresholds. Therefore, $\bar{\delta}_i$ denotes the average error detection probability for the warden, when it receives the signal transmitted from anchor a_i and uses the optimal threshold to detect.

D. Optimal Detection Threshold for the Warden

With the definition of ACP, we need to determine the optimal thresholds for the warden to separately detect anchors' signals with two different noise power distribution models. From the warden's perspective, it is desired to minimize the average error detection probability $T(\gamma_i)$, i.e.,

$$T(\gamma_i) = \int_{-\infty}^\infty \delta_i(\sigma_w^2, \gamma_i) f_{\sigma_w^2}(\sigma_w^2) d\sigma_w^2 \qquad (14)$$

where $f_{\sigma_w^2}(\cdot)$ denotes $f_{\sigma_w^2}^{BUM}(\cdot)$ or $f_{\sigma_w^2}^{UUM}(\cdot)$.

Proposition 1: With BUM, from the warden's perspective, the optimal threshold to detect the signal transmitted from anchor a_i is

$$\gamma_i^* = \mathrm{argmin}_{\gamma_i} T(\gamma_i)|_{f_{\sigma_w^2}(\sigma_w^2) = f_{\sigma_w^2}^{BUM}(\sigma_w^2)}$$

$$= \mathrm{argmin}_{\gamma_i} \int_{\frac{1}{\rho}\sigma_n^2}^{\rho\sigma_n^2} \delta_i(\sigma_w^2, \gamma_i) f_{\sigma_w^2}^{BUM}(\sigma_w^2) d\sigma_w^2$$

$$= P_{i,w}^r + \frac{1}{\rho}\sigma_n^2. \qquad (15)$$

Proof: See Appendix A. ∎

With UUM, due to the complicated expression of the probability density function in (5), we approximate $f_{\sigma_w^2}^{UUM}(\sigma_w^2)$ by a Gaussian function $\hat{f}_{\sigma_w^2}^{UUM}(\sigma_w^2)$, which is similar to [28], i.e.,

$$f_{\sigma_w^2}^{UUM}(\sigma_w^2) \approx \hat{f}_{\sigma_w^2}^{UUM}(\sigma_w^2)$$

$$= \frac{1}{\sqrt{2\pi\mu_2}\mu_3}\exp\left(-\frac{(\sigma_w^2 - \mu_1)^2}{2\mu_2}\right), \quad \sigma_w^2 > 0, \qquad (16)$$

where μ_1 and μ_2 are given below (5), and $\mu_3 = 0.5\left(1 - \mathrm{erf}\left(-\frac{\mu_1}{\sqrt{2\mu_2}}\right)\right) > 0$.

Based on the above approximated power distribution, we have the following Proposition 2 to describe the approximated optimal threshold value for the warden.

Proposition 2: With UUM, from the warden's perspective, the optimal threshold to detect the signal transmitted from anchor a_i is

$$\gamma_i^* = \mathrm{argmin}_{\gamma_i} T(\gamma_i)|_{f_{\sigma_w^2}(\sigma_w^2) = \hat{f}_{\sigma_w^2}^{UUM}(\sigma_w^2)}$$

$$= \mathrm{argmin}_{\gamma_i} \int_0^\infty \delta_i(\sigma_w^2, \gamma_i) \hat{f}_{\sigma_w^2}^{UUM}(\sigma_w^2) d\sigma_w^2$$

$$= \max\left\{\frac{P_{i,w}^r}{2} + \mu_1, P_{i,w}^r\right\}. \qquad (17)$$

Proof: See Appendix B. ∎

IV. LOCALIZATION ACCURACY METRICS FOR THE AGENT

In this section, we first introduce the metric for measuring the localization accuracy of the agent when the warden does not exist. Then, in the presence of the illegitimate warden, covert SPEB (CSPEB) is introduced to measure the localization accuracy when the ACPs satisfy the covertness requirement.

A. Squared Position Error Bound (SPEB)

We first focus on the scenario in the absence of the warden. The mean square error (MSE) of the agent's position estimation is bounded by the squared position error bound (SPEB) [36],

$$\mathcal{P}(b) = \mathrm{tr}\{J(b)^{-1}\}. \qquad (18)$$

Due to the fact that the unknown parameter in our model only consists of the position of the agent, Fisher information matrix (FIM), $J(b)$, can be expressed as

$$J(b) = \sum_{i=1}^N \lambda_i J_r(\phi_i), \qquad (19)$$

where $J_r(\phi_i)$ is called the ranging direction matrix (RDM),

$$J_r(\phi_i) = \begin{pmatrix} \cos^2(\phi_i) & \cos(\phi_i)\sin(\phi_i) \\ \cos(\phi_i)\sin(\phi_i) & \sin^2(\phi_i) \end{pmatrix}, \qquad (20)$$

where ϕ_i is the angle-of-arrival from anchor a_i to the agent. In (19), λ_i is the ranging information intensity (RII), and is defined in multipath scene as [36]

$$\lambda_i = \frac{8\pi^2\beta^2}{c^2}(1 - \chi_i)SNR_i^1, \qquad (21)$$

where β is the effective bandwidth of signal [36] and χ_i is the path-overlap coefficient. Note that, SNR_i^1 is the SNR of the first path in the received signal transmitted from a_i,

$$SNR_i^1 = \frac{|A_i|^2 \int_{-\infty}^{+\infty}|S(f)|^2 df}{N_0}, \qquad (22)$$

where A_i denotes the amplitude of the received signal and equals to $\sqrt{\frac{A^\circ P_i^t}{d_{i,b}^\varrho}}$. With the assumption that signals experience LOS channels, i.e., $\chi_i = 0$, we have [38]

$$\lambda_i = \xi_i \frac{P_i^t}{d_{i,b}^\varrho}, \qquad (23)$$

where ξ_i is a positive coefficient determined by the channel property and the effective bandwidth of the transmitted signal. Obviously, for signals received by the agent, A^o is included in ξ_i.

Proposition 3: For a given localization geometry, namely the positions of anchors and the agent are fixed, SPEB is convex and non-increasing in $\boldsymbol{\lambda}$, where $\boldsymbol{\lambda} = (\lambda_1, \lambda_2, \cdots, \lambda_N)^T$.

The proof of Proposition 3 can refer to the properties of SPEB in [2]. It implies that, for fixed ξ_i and $d_{i,b}^\varrho$, increasing the power of the signals transmitted from the anchor network results in better localization performance for the agent.

B. Covert SPEB (CSPEB)

When the warden exists, the legitimate anchors and agent will introduce a covertness requirement coefficient ϵ to measure the probability that the localization signals are not detected. The coefficient $\epsilon \in (0,1)$ signifies the covertness requirement, and a sufficiently small ϵ renders any detector employed by the warden to be ineffective [24]. Obviously, SPEB cannot characterize the connection between the covertness requirement coefficient ϵ and the localization accuracy. Therefore, we introduce the CSPEB, which is the lower bound of localization accuracy for the agent that takes into account the covertness requirement coefficient. Namely, the CSPEB $\mathcal{P}_C(\boldsymbol{b})$ is to describe the SPEB for the agent, in the case that ACPs of anchor network satisfy $\bar{\delta}_i \geq 1 - \epsilon$, $\forall i \in \mathcal{N}_a$.

V. PERFORMANCE ANALYSIS OF COVERT LOCALIZATION WITH NOISE UNCERTAINTY DISTRIBUTIONS

In this section, we first formulate the basic optimization problem from the perspective of the legitimate agent and anchors to achieve covert localization. The problem aims to solve the optimal transmit powers of anchors to minimize the localization accuracy bound while satisfying the covert requirement constraint. The CSPEB is obtained after getting the maximum available transmit power of anchors, and then the factors that affect the covert localization performance are analyzed. Moreover, the robust optimization problem is formulated in the presence of the warden's position uncertainty. Besides, in an energy-constrained localization scenario, we explore the power allocation strategy of anchors in the presence of the total power constraint.

A. The Basic Optimization Problem and Solutions

If the warden can obtain the power values of the received signals and know the experienced noise uncertainty distribution, from its perspective, the warden must use the optimal thresholds γ_i^* in (15) or (17) to separately detect the localization signals. For the agent and anchors, the essential requirement is to minimize localization errors while ensuring covertness from the warden. Therefore, the basic optimization problem for covert localization is

$$\mathscr{P}: \quad \underset{\boldsymbol{P}}{\text{minimize}} \ \mathcal{P}(\boldsymbol{b}) \tag{24}$$

$$\text{s.t. } \bar{\delta}_i \geq 1 - \epsilon, \quad \forall i \in \mathcal{N}_a, \tag{25}$$

where $\boldsymbol{P} = \{P_1^t, P_2^t, \cdots, P_N^t\}$ is the transmit power vector of the anchors. In the case that anchors transmit signal according

to the solved transmit power values, the warden cannot perfectly detect localization signals with error probability $1 - \epsilon$, while the agent can obtain the CSPEB.

Theorem 1: With BUM, when the warden separately detects signals that transmitted from anchor network by the optimal thresholds $\gamma_i^*, \forall i \in \mathcal{N}_a$, the CSPEB for the agent is

$$\mathcal{P}_C^{BUM}(\boldsymbol{b}) = \frac{A^o}{(\rho^{2\epsilon-1} - \frac{1}{\rho})\sigma_n^2} \left(\sum_{i=1}^N \left(\frac{d_{i,w}}{d_{i,b}} \right)^\varrho \xi_i \boldsymbol{J}_r(\phi_i) \right)^{-1}. \tag{26}$$

Proof: Substituting γ_i^* of BUM into (13), it derives

$$\bar{\delta}_i = \int_{\frac{1}{\rho}\sigma_n^2}^{\rho\sigma_n^2} \delta_i(\sigma_w^2, \gamma_i^*) f_{\sigma_w^2}^{BUM}(\sigma_w^2) \mathrm{d}\sigma_w^2$$

$$= \frac{1}{2\ln(\rho)} \ln \left(\frac{\rho\sigma_n^2}{P_{i,w}^r + \frac{1}{\rho}\sigma_n^2} \right). \tag{27}$$

With the constraint in $\mathscr{P}$, we can obtain the maximum power of received signal from $\boldsymbol{a}_i$, i.e.,

$$P_{i,w}^r = \left(\rho^{2\epsilon-1} - \frac{1}{\rho} \right) \sigma_n^2, \tag{28}$$

the corresponding maximum transmit power of signal transmitted from $\boldsymbol{a}_i$ is

$$P_i^t = \frac{P_{i,w}^r d_{i,w}^\varrho}{A^o} = \left(\rho^{2\epsilon-1} - \frac{1}{\rho} \right) \frac{\sigma_n^2 d_{i,w}^\varrho}{A^o}, \tag{29}$$

and the maximum RII provided by anchor $\boldsymbol{a}_i$ is

$$\lambda_i = \left(\rho^{2\epsilon-1} - \frac{1}{\rho} \right) \left(\frac{d_{i,w}}{d_{i,b}} \right)^\varrho \frac{\xi_i \sigma_n^2}{A^o}. \tag{30}$$

Substituting $\lambda_i, \forall i \in \mathcal{N}_a$ into (18) and (19), we can obtain the CSPEB in the case of BUM. ∎

Remark 1: In Theorem 1, the CSPEB of the agent is related to the noise uncertainty parameter, the covertness requirement coefficient, the distance between anchors and the warden, the characteristics of transmissions, and the localization geometry between anchors and the agent. We draw the following observations from Theorem 1.

- The covertness requirement coefficient ϵ is essential to assess and balance the localization accuracy and covert performance. The first derivative of $\rho^{2\epsilon-1} - \frac{1}{\rho}$ with respect to ϵ is $\frac{\partial}{\partial\epsilon}(\rho^{2\epsilon-1} - \frac{1}{\rho}) = 2\rho^{2\epsilon-1}\ln(\rho)$. Thus, we have $\frac{\partial}{\partial\epsilon}(\rho^{2\epsilon-1} - \frac{1}{\rho}) \geq 0$, for $\forall\epsilon \in (0,1)$ and $\forall\rho \geq 1$, which means that $\mathcal{P}_C^{BUM}(\boldsymbol{b})$ decreases with the covertness requirement coefficient ϵ. Namely, in order to achieve a better covertness to the warden, anchors should transmit signals with lower power, while the agent's localization accuracy will be worse.
- The noise uncertainty parameter ρ is to quantify the noise uncertainty in BUM, and can be operated to achieve a specific purpose. Mathematically, the first derivative of $\rho^{2\epsilon-1} - \frac{1}{\rho}$ with respect to ρ is $\frac{\partial}{\partial\rho}(\rho^{2\epsilon-1} - \frac{1}{\rho}) = \rho^{-2}\left(\rho^{2\epsilon}(2\epsilon-1) + 1\right)$. On one hand, when $\epsilon < 0.5$,

we have

$$\frac{\left(\rho^{2\epsilon}(2\epsilon-1)+1\right)}{\rho^2} = \begin{cases} > 0, & \text{if } 1 \le \rho < (1-2\epsilon)^{-\frac{1}{2\epsilon}}, \\ = 0, & \text{if } \rho = (1-2\epsilon)^{-\frac{1}{2\epsilon}}, \\ < 0, & \text{if } \rho > (1-2\epsilon)^{-\frac{1}{2\epsilon}}. \end{cases} \tag{31}$$

Thus, when $\epsilon < 0.5$ and $1 \le \rho < (1-2\epsilon)^{-\frac{1}{2\epsilon}}$, $\rho^{2\epsilon-1} - \frac{1}{\rho}$ monotonically increases with respect to ρ and CSPEB $\mathcal{P}_C^{BUM}(\boldsymbol{b})$ monotonically decreases with respect to ρ. When $\epsilon < 0.5$ and $\rho > (1-2\epsilon)^{-\frac{1}{2\epsilon}}$, $\rho^{2\epsilon-1} - \frac{1}{\rho}$ monotonically decreases with respect to ρ and CSPEB $\mathcal{P}_C^{BUM}(\boldsymbol{b})$ monotonically increases with respect to ρ. When $\epsilon < 0.5$ and $\rho = (1-2\epsilon)^{-\frac{1}{2\epsilon}}$, $\rho^{2\epsilon-1} - \frac{1}{\rho}$ reaches its maximum value, while CSPEB $\mathcal{P}_C^{BUM}(\boldsymbol{b})$ achieves its minimum value. On the other hand, when $\epsilon > 0.5$, $\rho^{-2}\left(\rho^{2\epsilon}(2\epsilon-1)+1\right) > 0$, $\rho^{2\epsilon-1} - \frac{1}{\rho}$ monotonically increases with respect to ρ, and CSPEB $\mathcal{P}_C^{BUM}(\boldsymbol{b})$ monotonically decreases with respect to ρ.

- The nominal noise power σ_n^2 and distances between the warden and each anchor $d_{i,w}, \forall i \in \mathcal{N}_a$ also have an effect on CSPEB $\mathcal{P}_C^{BUM}(\boldsymbol{b})$. It is obvious that CSPEB is inversely proportional to σ_n^2. In addition, CSPEB $\mathcal{P}_C^{BUM}(\boldsymbol{b})$ is non-increasing as $d_{i,w}^\varrho$ increases, which indicates that investigating the warden in near-field and far-field cases is meaningful.

Corollary 1: With BUM, when the covertness requirement coefficient $\epsilon < 0.5$, i.e., the warden's average covert probability for anchor $\boldsymbol{a}_i, \forall i \in \mathcal{N}_a$, satisfies $0.5 < \bar{\delta}_i < 1$, the CSPEB has its minimum value when the noise uncertainty parameter is

$$\rho = (1-2\epsilon)^{-\frac{1}{2\epsilon}}. \tag{32}$$

Thus, with a fixed nominal noise power, a larger noise uncertainty parameter for the warden may not result in a better covert localization accuracy for the agent.

Theorem 2: With UUM, when the warden detects signals by the optimal thresholds $\gamma_i^*, \forall i \in \mathcal{N}_a$, the maximum transmit power of anchor $\boldsymbol{a}_i$ to satisfy $\bar{\delta}_i \ge 1 - \epsilon$ is

$$P_i^t = \begin{cases} 2\sqrt{2\mu_2}\frac{d_{i,w}^\varrho}{A^o}\text{erf}^{-1}(\epsilon\mu_3), & \text{if } \epsilon < \frac{\mu_4}{\mu_3}, \\ \mu_1\frac{d_{i,w}^\varrho}{A^o} + \sqrt{2\mu_2}\frac{d_{i,w}^\varrho}{A^o}\text{erf}^{-1}\left(2\mu_3\epsilon - \mu_4\right), & \text{otherwise}, \end{cases} \tag{33}$$

where $\mu_4 = \text{erf}(\frac{\mu_1}{\sqrt{2\mu_2}})$. Meanwhile, the corresponding CSPEB $P_C^{UUM}(\boldsymbol{b})$ is

$$P_C^{UUM}(\boldsymbol{b})$$
$$= \begin{cases} \frac{A^o\left(\sum_{i=1}^N \left(\frac{d_{i,w}}{d_{i,b}}\right)^\varrho \xi_i \boldsymbol{J}_r(\phi_i)\right)^{-1}}{2\sqrt{2\mu_2}\text{erf}^{-1}(\epsilon\mu_3)}, & \text{if } \epsilon < \frac{\mu_4}{\mu_3}, \\ A^o\left(\mu_1 + \sqrt{2\mu_2}\text{erf}^{-1}\left(2\mu_3\epsilon - \mu_4\right)\right)^{-1} \\ \cdot \left(\sum_{i=1}^N \left(\frac{d_{i,w}}{d_{i,b}}\right)^\varrho \xi_i \boldsymbol{J}_r(\phi_i)\right)^{-1}, & \text{otherwise}. \end{cases} \tag{34}$$

Proof: See Appendix B. ∎

Remark 2: From (34), the CSPEB of the agent is related to the noise uncertainty parameter $\sigma_{\Delta,\text{dB}}^2$, through μ_1, μ_2,

and μ_3, the covertness requirement coefficient ϵ, distances between anchors and the warden, the characteristics of transmissions ξ_i, and the localization geometry between anchors and the agent. From Theorem 2, we have the following observations.

- Similar to the case in BUM, CSPEB $\mathcal{P}_C^{UUM}(\boldsymbol{b})$ decreases with the covertness requirement coefficient ϵ.
- Different from BUM, CSPEB $\mathcal{P}_C^{UUM}(\boldsymbol{b})$ monotonically decreases with the noise uncertainty coefficient $\sigma_{\Delta,\text{dB}}^2$, regardless of the value of $\sigma_{\Delta,\text{dB}}^2$.
- With UUM, CSPEB $\mathcal{P}_C^{UUM}(\boldsymbol{b})$ decreases with the nominal noise power $\sigma_{n,\text{dB}}^2$ of the warden.

The detailed derivations and analysis of Remark 2 are shown in Appendix C.

B. Localization Accuracy Analysis With the Warden's Position Uncertainty

This subsection provides the worst-case CSPEB in the presence of the warden's position uncertainty. The optimization problem should be modified as

$$\mathscr{P}^R: \quad \underset{\boldsymbol{P}}{\text{minimize}} \; \tilde{\mathcal{P}}(\boldsymbol{b}) \tag{35}$$
$$\text{s.t. } \bar{\delta}_i \ge 1 - \epsilon, \quad \forall i \in \mathcal{N}_a, \tag{36}$$
$$\tilde{\boldsymbol{w}} \in \mathscr{C}(\boldsymbol{w}, \Delta w), \tag{37}$$

where $\mathscr{C}(\boldsymbol{w}, \Delta w)$ is used to describe the warden's position uncertainty area, shown in Fig. 2. The objective $\tilde{\mathcal{P}}(\boldsymbol{b}) = \max_{\Delta w}(\mathcal{P}(\boldsymbol{b}))$ is to describe the worst-case localization accuracy for the agent when the warden's position is uncertain.

Since anchors only know the potential area rather than the exact position of the warden, they must transmit signals with proper power to guarantee that the localization signals are covert to the warden. For each anchor, the uncertain distance with the warden is given in (6). To achieve covertness, anchor $\boldsymbol{a}_i$ must consider that the warden is likely to locate at the closest position with minimum distance, i.e., $\min \tilde{d}_{i,w} = d_{i,w} - \Delta w$.

Then, we give the expressions of the worst-case CSPEBs. With BUM, the maximum transmit power of the signal transmitted from anchor $\boldsymbol{a}_i$ is

$$\tilde{P}_i^t = \left(\rho^{2\epsilon-1} - \frac{1}{\rho}\right)\frac{\sigma_n^2(d_{i,w} - \Delta w)^\varrho}{A^o}, \tag{38}$$

and the worst-case CSPEB for the agent in BUM is

$$\tilde{\mathcal{P}}_C^{BUM}(\boldsymbol{b}) = \frac{A^o\left(\sum_{i=1}^N \left(\frac{(d_{i,w}-\Delta w)}{d_{i,b}}\right)^\varrho \xi_i \boldsymbol{J}_r(\phi_i)\right)^{-1}}{(\rho^{2\epsilon-1} - \frac{1}{\rho})\sigma_n^2}. \tag{39}$$

Similarly, with UUM, the maximum transmit power of the signal transmitted from $\boldsymbol{a}_i$ is

$$\tilde{P}_i^t = \begin{cases} 2\sqrt{2\mu_2}\frac{(d_{i,w}-\Delta w)^\varrho}{A^o}\text{erf}^{-1}(\epsilon\mu_3), & \text{if } \epsilon < \frac{\mu_4}{\mu_3}, \\ \mu_1\frac{(d_{i,w}-\Delta w)^\varrho}{A^o} \\ +\sqrt{2\mu_2}\frac{(d_{i,w}-\Delta w)^\varrho}{A^o}\text{erf}^{-1}\left(2\mu_3\epsilon - \mu_4\right), & \text{otherwise}, \end{cases} \tag{40}$$

and the worst-case CSPEB for the agent $\tilde{P}_C^{UUM}(\boldsymbol{b})$ in UUM is

$$
\begin{aligned}
&\tilde{P}_C^{UUM}(\boldsymbol{b}) \\
&= \begin{cases}
\dfrac{A^o \left(\sum_{i=1}^N \left(\frac{d_{i,w}-\Delta w}{d_{i,b}} \right)^\varrho \xi_i \boldsymbol{J}_r(\phi_i) \right)^{-1}}{2\sqrt{2\mu_2}\mathrm{erf}^{-1}(\epsilon\mu_3)}, & \text{if } \epsilon < \frac{\mu_4}{\mu_3}, \\[12pt]
A^o \left(\mu_1 + \sqrt{2\mu_2}\mathrm{erf}^{-1}\left(2\mu_3\epsilon - \mu_4 \right) \right)^{-1} \\
\cdot \left(\sum_{i=1}^N \left(\frac{d_{i,w}-\Delta w}{d_{i,b}} \right)^\varrho \xi_i \boldsymbol{J}_r(\phi_i) \right)^{-1}, & \text{otherwise.}
\end{cases}
\end{aligned}
\tag{41}
$$

Remark 3: With BUM, with (38), the first derivative of $\tilde{P}_i^t$ with respect to Δw is $\frac{\partial \tilde{P}_i^t}{\partial \Delta w} = -\left(\rho^{2\epsilon-1} - \frac{1}{\rho} \right) \frac{\sigma_n^2}{A^o} \varrho(d_{i,w} - \Delta w)^{\varrho-1}$. In our scenario, the warden's position uncertainty makes sense when $\Delta w < d_{i,w}$, and results in $\frac{\partial \tilde{P}_i^t}{\partial \Delta w} < 0$. Thus, $\tilde{P}_i^t$ monotonically decreases with Δw, and $\mathcal{P}_C^{BUM}(\boldsymbol{b})$ increases with Δw. Besides, we can obtain the same conclusion in UUM, and the detailed derivations are omitted.

C. Power Allocation Strategy in Covert Localization

In the energy-constrained localization scenario, the total power of the anchor network is always limited [39]. Therefore, the power allocation strategy for anchors is required to minimize the localization error of the agent, constraining both the covert requirement and the total transmit power. The power allocation problem for covert localization can be formulated as

$$
\mathscr{P}^A : \ \underset{\boldsymbol{P}}{\text{minimize}}\, \mathcal{P}(\boldsymbol{b}) \tag{42}
$$

$$
\text{s.t. } \bar{\delta}_i \geq 1 - \epsilon, \quad \forall i \in \mathcal{N}_a, \tag{43}
$$

$$
\sum_{i \in \mathcal{N}_a} P_i^t \leq P_{\text{total}}, \tag{44}
$$

where P_{total} is the upper bound of the sum of anchors' powers. Since the covert requirement has restricted a maximum power constraint, there is no extra maximum power constraint. The goal of $\mathscr{P}^A$ is to find the optimal transmit power allocation strategy to minimize the CSPEB, while the anchors are covert for the warden and the powers satisfy the constraints.

Comparing $\mathscr{P}$ and $\mathscr{P}^A$, it is nontrivial to resolve the transmit powers of anchors owing to the total power constraint in (44). Theoretically, if the sum of maximum available powers in (29) or (33) is smaller than P_{total}, the CSPEBs in both the energy-constrained scenario and the basic scenario should be identical. On the contrary, the CSPEB in the energy-constrained scenario will be higher than the CSPEB in the basic scenario, because the anchors cannot consume as much energy as possible when the error probability constraint is met.

With (19), FIM $\boldsymbol{J}(\boldsymbol{b})$ is a linear function with respect to the power allocation vector $\boldsymbol{P}$ and (44) is a convex constraint. The constraint $\bar{\delta}_i \geq 1 - \epsilon, \forall i \in \mathcal{N}_a$, is equivalent to regarding the solved power (i.e., $(P_i^t)_{\max}$) in $\mathscr{P}$ as the upper bound of anchors' signal, namely, $P_i^t \leq (P_i^t)_{\max}, \forall i \in \mathcal{N}_a$. Therefore, by using the Schur complement and introducing a maximum power constraint that meets the covertness, $\mathscr{P}^A$ can

be transformed as a SDP [40], i.e.,

$$
\mathscr{P}^{A-SDP} : \ \underset{\boldsymbol{P},\boldsymbol{Y}}{\text{minimize}}\, \mathrm{tr}\{\boldsymbol{Y}\} \tag{45}
$$

$$
\text{s.t. } P_i^t \leq (P_i^t)_{\max}, \quad \forall i \in \mathcal{N}_a, \tag{46}
$$

$$
\sum_{i \in \mathcal{N}_a} P_i^t \leq P_{\text{total}}, \tag{47}
$$

$$
\begin{bmatrix} \boldsymbol{Y} & \boldsymbol{I} \\ \boldsymbol{I} & \sum_{i=1}^N \xi_i \frac{P_i^t}{d_{i,b}^\varrho} \boldsymbol{J}_r(\phi_i) \end{bmatrix} \succeq \boldsymbol{0}, \tag{48}
$$

where $\boldsymbol{Y}$ is an auxiliary matrix and has the same dimension with $\boldsymbol{J}(\boldsymbol{b})$. Now, in $\mathscr{P}^{A-SDP}$, all the objective and constraints are convex with respect to the unknown variables, i.e., $\boldsymbol{P}$ and $\boldsymbol{Y}$. The interior-point method can be utilized to efficiently approach the SDP $\mathscr{P}^{A-SDP}$.

VI. SIMULATION RESULTS AND DISCUSSIONS

In this section, we present simulation results to examine and illustrate our theoretical analysis of covert localization.

A. Network Settings for Simulations

This subsection presents the localization network settings, including positions of network nodes and the transmission channel parameters. The anchor network consists of $N = 8$ stationary anchors located at the boundary of a square area $[0, 300] \times [0, 300]\text{m}^2$, i.e., $\boldsymbol{a}_1 = [100, 0]^T$, $\boldsymbol{a}_2 = [200, 0]^T$, $\boldsymbol{a}_3 = [300, 100]^T$, $\boldsymbol{a}_4 = [300, 200]^T$, $\boldsymbol{a}_5 = [200, 300]^T$, $\boldsymbol{a}_6 = [100, 300]^T$, $\boldsymbol{a}_7 = [0, 200]^T$, $\boldsymbol{a}_8 = [0, 100]^T$. Except for specific instructions and comparisons, the position of the agent is $\boldsymbol{b} = [400, 200]^T$, the position of the warden is $\boldsymbol{w} = [400, 300]^T$, and the nominal noise power $\sigma_{n,\text{dB}}^2 = -50\text{dB}$ in both BUM and UUM. To make results intuitive, we deliberately restrict our attention to the accuracy analysis of covert localization to gain insights, rather than the channel modeling and signal design as well as identification. Hence, the coefficient ξ_i, which indicates the channel property and the effective bandwidth of the transmitted signal, follows uniform distribution $\xi_i \sim U[0, 100]$, while the channel gain $A^o = 0.0001$.

B. Accuracy of Covert Localization

We investigate the effect of covertness requirement coefficient (ϵ) and noise uncertainty parameter (ρ, or $\sigma_{\Delta,\text{dB}}^2$) on the covert localization accuracy for the agent. We first validate Corollary 1 that CSPEB does not monotonically decrease with respect to ρ when ϵ is less than 0.5 and the minimum point is $\rho = (1 - 2\epsilon)^{-\frac{1}{2\epsilon}}$. Fig. 3 shows the CSPEB comparison with varying ρ when ϵ equals to 0.001 and 0.6, respectively. Obviously, CSPEB is not monotonic with respect to ρ when $\epsilon = 0.001 < 0.5$, and reaches its minimum value at $\rho = (1 - 2\epsilon)^{-\frac{1}{2\epsilon}}|_{\epsilon=0.001} = 2.7210$. This result is consistent with Corollary 1. In contrast, CSPEB monotonically decreases with respect to ρ when $\epsilon = 0.6 > 0.5$. From anchors' perspective, the smaller the covertness requirement coefficient ϵ, the more advantageous it is for covert localization. However, a larger noise uncertainty coefficient ρ may not result in better covert localization accuracy. Thus, it is essential to
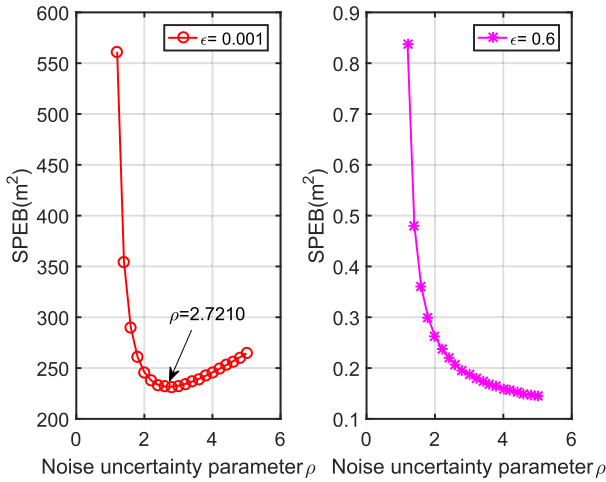
Fig. 3. CSPEB versus noise uncertainty parameter ρ when ϵ equals to 0.001 and 0.6 respectively in BUM.
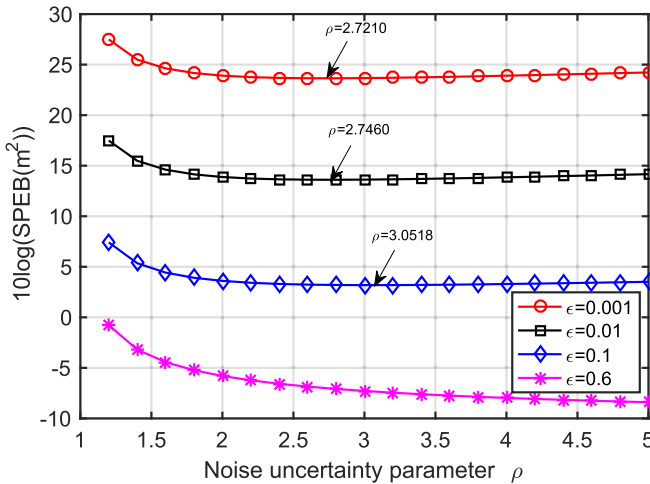
Fig. 4. CSPEB versus noise uncertainty parameter ρ with different covertness requirement coefficient ϵ in BUM.

dynamically adjust the delicate relationship between ρ and ϵ to achieve a specific covertness purpose according to Corollary 1.

Fig. 4 and Fig. 5 compare the CSPEB with respect to varying noise uncertainty parameter and multiple covertness requirement coefficients ϵ in BUM and UUM, respectively. From these two figures, we can draw the following observations. First, covertness requirement coefficient ϵ increases the CSPEB in both models, since anchors must transmit signals with less powers to ensure that localization signals are not detected by the warden. Second, with BUM, CSPEB monotonically decreases with ρ when $\epsilon > 0.5$, but has the minimum values at $\rho = (1 - 2\epsilon)^{-1/(2\epsilon)}$ when $\epsilon < 0.5$. With UUM, CSPEB is a monotonically decreasing function of noise uncertainty parameter $\sigma_{\Delta,\mathrm{dB}}^2$. Namely, in UUM, from the perspective of the anchors and the agent, the covert localization accuracy can be improved by enhancing the noise uncertainty that the warden experiences, but this manner is not held in BUM.

C. Effect of the Warden's Position Uncertainty

We evaluate the worst-case CSPEB for the agent in the existence of the warden's position uncertainty. Both BUM and
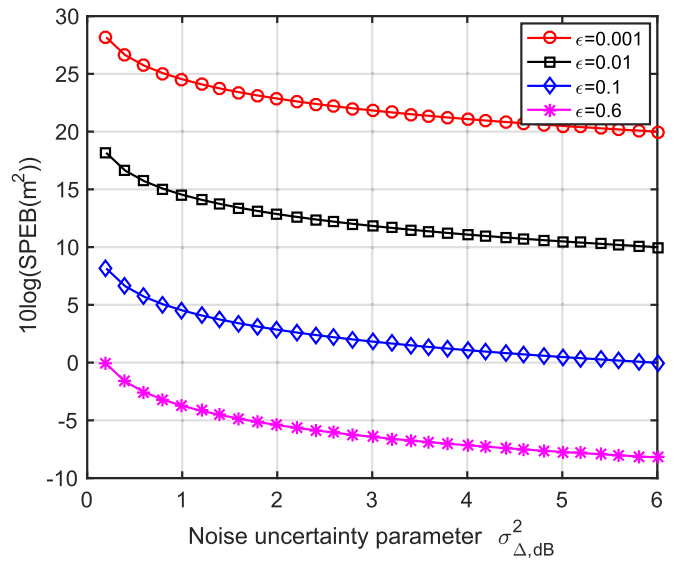
Fig. 5. CSPEB versus noise uncertainty parameter $\sigma_{\Delta,\mathrm{dB}}^2$ with different covertness requirement coefficient ϵ in UUM.

TABLE I
GROUPS OF THE AGENT $\boldsymbol{b}$ AND THE WARDEN $\boldsymbol{w}$

	Group 1	Group 2	Group 3	Group 4
$\boldsymbol{b}$	[400, 200]	[400, 200]	[600, 400]	[600, 400]
$\boldsymbol{w}$	[400, 300]	[600, 500]	[400, 300]	[600, 500]

UUM scenarios are evaluated in Fig. 6(a) and Fig. 6(b), respectively. In these two figures, we set the covertness requirement coefficient $\epsilon = 0.001$, while the radius of the warden's position uncertainty area equals to $0, 10, 30, 50$, respectively. We can see that the CSPEB decreases with Δw in these two models. This means that if the warden's position can be estimated more accurately, the agent can achieve a better covert localization accuracy. The worst-case CSPEB is derived based on the robust optimization technique and provides a fundamental limit no matter where the warden is located within its uncertainty region. Different conclusions may be attained if the distribution of the warden in its uncertainty region is employed. It is worth mentioning that the minimum value of CSPEB in BUM is related to ρ and ϵ, so that CSPEBs with different Δw obtain their minimum value at the same point of noise uncertainty coefficient.

D. Near-Field and Far-Field Localization

We use four groups of agents and wardens to investigate the near-field and far-field localization accuracy. The particular positions of agents and wardens are shown in Table I. In this part, we assume the position of the warden is known, and the covertness requirement coefficient is $\epsilon = 0.001$. Fig. 7(a) and Fig. 7(b) show the comparisons of CSPEBs in both BUM and UUM. First, the sequence of CSPEBs corresponding to different groups in these two figures is identical regardless of the noise uncertainty models. Specifically, comparing Groups 1 and 3 (or Groups 2 and 4), the position of the warden is the same, while the agent is far away from the anchors in the latter group. The distances and geometries between the anchors and

(a) BUM

(b) UUM
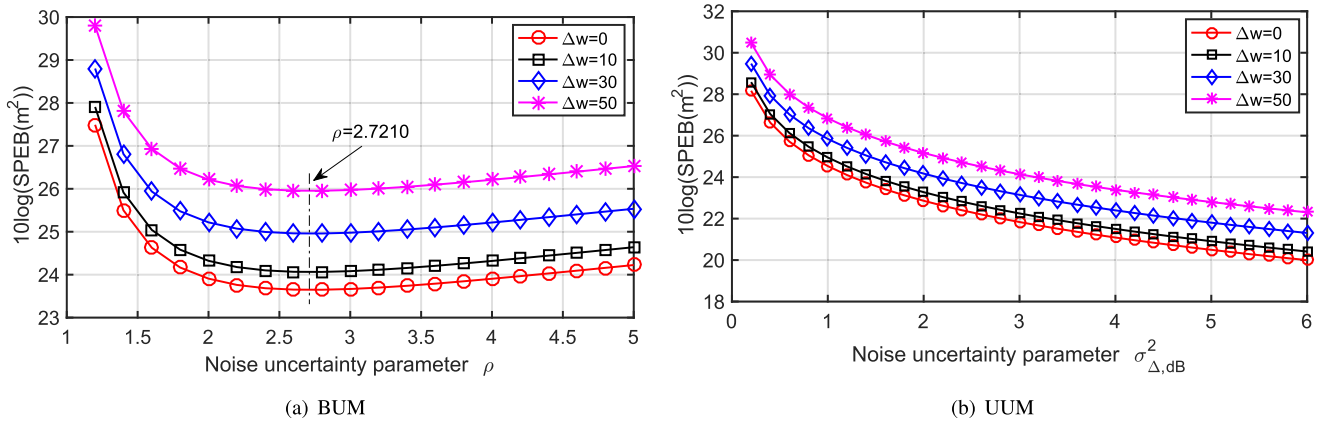
Fig. 6.   The worst-case CSPEB versus noise uncertainty parameter ρ or $\sigma^2_{\Delta,\mathrm{dB}}$ with different warden's position uncertainty Δw.

(a) BUM

(b) UUM
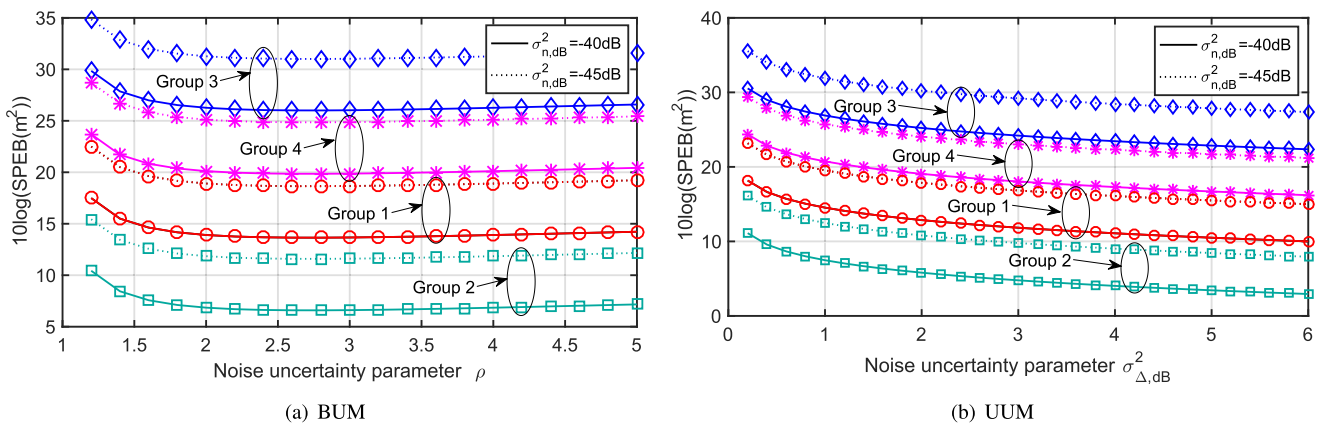
Fig. 7.   CSPEB versus noise uncertainty parameter ρ or $\sigma^2_{\Delta,\mathrm{dB}}$ with different groups (Groups 1-4) of agent and warden and nominal noise power $\sigma^2_{n,\mathrm{dB}}$.

the agent result in the difference of CSPEBs. Second, Group 2 has the lowest CSPEB because anchors can transmit signals by using higher power since the warden is far from the anchor network. In contrast, Group 3 has the highest CSPEB since the warden is close to the anchor network.

E. Levels of Nominal Background Noise

In some cases, due to the friendly interference or cooperative jamming as well as artificial noise, the background noise level around the warden may also be variable and controllable. We then evaluate the covert localization accuracy with respect to two different nominal noise power values, i.e., $\sigma^2_{n,\mathrm{dB}}$ equals to -40dB and -45dB respectively. Previous four groups are still used and the covertness requirement coefficient ϵ is equal to 0.001. The comparisons of CSPEBs in both BUM and UUM are evaluated in Fig. 7(a) and Fig. 7(b), respectively. We can see from these figures that, CSPEBs increase with the nominal noise power for the warden, indicating that the nominal noise power has a significant impact on signal detection and covert localization accuracy of the agent for both BUM and UUM. Besides, compared the CSPEBs of Group 3 with $\sigma^2_{n,\mathrm{dB}} = -40$dB and Group 4 with $\sigma^2_{n,\mathrm{dB}} = -45$dB, it implies that the network geometry and the level of the nominal background noise can be complementary to achieve covert localization with a certain covertness requirement.

F. Power Allocation Solutions

To evaluate the performance of the SDP-based algorithm when solving the power allocation problem $\mathscr{P}^{\mathrm{A}}$, we explicitly compare it with two other approaches. These two straightforward schemes perform based on the constraints and serve as the baselines, i.e., proportional reduction power allocation (PRPA) method and random allocation and recompensation (RAR) method. With PRPA, based on the solution of $\mathscr{P}$ in (29) and (33), if $P_{\mathrm{total}} \leq \sum_{i=1}^{N}(p_i^t)_{\max}$, the allocated power of anchor $\boldsymbol{a}_i$ is $\check{p}_i^t = \frac{(p_i^t)_{\max}}{\sum_{i=1}^{N}(p_i^t)_{\max}} P_{\mathrm{total}}$; otherwise, $\check{p}_i^t = (p_i^t)_{\max}$. There are two steps of RAR method. In the first step, the allocated power of anchor $\boldsymbol{a}_i$ is $\hat{p}_i^t \sim U(0, (p_i^t)_{\max})$. In the second step, the extra power may be allocated again. If $P_{\mathrm{total}} \leq \sum_{i=1}^{N}(p_i^t)_{\max}$, $\hat{p}_i^t \leftarrow \hat{p}_i^t + \frac{\hat{p}_i^t}{\sum_{i=1}^{N}\hat{p}_i^t}(P_{\mathrm{total}} - \sum_{i=1}^{N}\hat{p}_i^t)$; otherwise, $\hat{p}_i^t \leftarrow \hat{p}_i^t + \frac{(p_i^t)_{\max} - \hat{p}_i^t}{\sum_{i=1}^{N}((p_i^t)_{\max} - \hat{p}_i^t)}(\sum_{i=1}^{N}(p_i^t)_{\max} - \sum_{i=1}^{N}\hat{p}_i^t)$.

The positions of the anchors, the agent, and the warden are the same as that of Section VI.A. The covertness requirement coefficient $\epsilon = 0.001$ and noise uncertainty parameter $\rho = (1 - 2\epsilon)^{-\frac{1}{2\epsilon}}|_{\epsilon=0.001}$ in BUM, and $\sigma^2_{\Delta,\mathrm{dB}} = 0.5$ in UUM. Note that the average CSPEB measures the performance of RAR method by using Monte Carlo method with 1000 trials. Fig. 8 depicts the CSPEB varying with respect to the total power for the anchor network in both BUM and UUM. First, in Fig. 8(a), the CSPEB without power constraint is constant
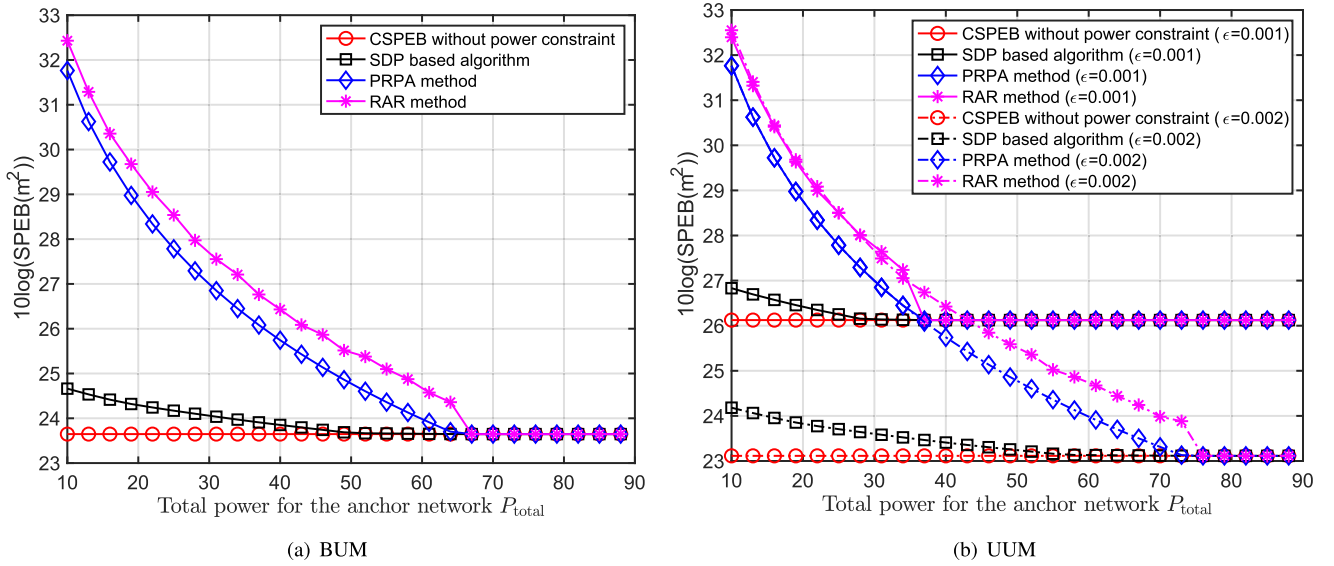
Fig. 8.   CSPEB versus the total available power for the anchor network P_{total}.

and gives the benchmark for power allocation solutions. Before these curves intersect, the sum of anchors' power is less than the total power so that the CSPEBs with constraint are far from the benchmark. Meanwhile, the SDP-based algorithm performs better than both the PRPA and RAR methods. Second, we can obtain the same result in Fig. 8(b) that the performance of the SDP-based algorithm is better than the other two methods. Third, in Fig. 8(b), the maximum power for each anchor becomes larger when the covertness requirement coefficient $\epsilon = 0.002$, which causes the curves' intersection to move to the right.

VII. Conclusion

In this paper, we have developed a framework to investigate covert localization to prevent the localization process from being detected by the warden. Specifically, we have demonstrated that noise uncertainty for the warden is beneficial for achieving covert localization. Based on the analysis of ACPs with BUM and UUM, we have proposed the CSPEB to measure the localization accuracy of the agent when the warden suffers noise uncertainty. Furthermore, we have investigated factors affecting CSPEB, including the covertness requirement coefficient, the noise uncertainty parameter, the warden's position uncertainty, the geometry of the network, and the nominal noise power. Besides, we have formulated a power allocation problem in covert localization, constraining the total power for the anchors and proposed a SDP-based algorithm to resolve it. Extensive simulations have been carried out to validate the theoretical analysis of the CSPEB. The results from this paper can be used as a guideline for the design of covert localization strategies, enabling security and energy-efficient localization networks.

For future work, we will extend the theoretical analysis of the covert localization to cooperative networks where multiple agents and friendly interference signals exist. Moreover, we will design covert schemes in localization networks to achieve specific purposes.

Appendix A
The Proof of Proposition 1

With BUM, substituting $f_{\sigma_w^2}^{BUM}(\sigma_w^2)$ into (14), we can obtain the average error detection probability with respect to γ_i, which can be expressed as a continuous piecewise function as

$$T(\gamma_i)$$
$$= \begin{cases} 1, & \text{if } \gamma_i < \frac{1}{\rho}\sigma_n^2, \\ \frac{1}{2\ln(\rho)}\ln\left(\frac{\rho\sigma_n^2}{\gamma_i}\right), & \text{if } \frac{1}{\rho}\sigma_n^2 \leq \gamma_i < P_{i,w}^r + \frac{1}{\rho}\sigma_n^2, \\ \frac{1}{2\ln(\rho)}\ln\left(1 - \frac{P_{i,w}^r}{\gamma_i}\right) + 1, & \text{if } P_{i,w}^r + \frac{1}{\rho}\sigma_n^2 \leq \gamma_i < \rho\sigma_n^2, \\ \frac{1}{2\ln(\rho)}\ln\left(\frac{(\gamma_i - P_{i,w}^r)\rho}{\sigma_n^2}\right), & \text{if } \rho\sigma_n^2 \leq \gamma_i < \rho\sigma_n^2 + P_{i,w}^r, \\ 1, & \text{if } \gamma_i \geq \rho\sigma_n^2 + P_{i,w}^r. \end{cases}$$
$$(49)$$

The warden will not set the detection threshold for the signal transmitted from anchor as $\gamma_i \leq \frac{1}{\rho}\sigma_n^2$ or $\gamma_i \geq \rho\sigma_n^2$, since $T(\gamma_i)$ is at the worst case. For $\frac{1}{\rho}\sigma_n^2 \leq \gamma_i < P_{i,w}^r + \frac{1}{\rho}\sigma_n^2$, we derive the first derivative of $T(\gamma_i)$ with respect to γ_i as

$$T'(\gamma_i) = -\frac{1}{2\gamma_i\ln(\rho)} < 0. \qquad (50)$$

This demonstrates that $T(\gamma_i)$ is a decreasing function of γ_i when $\frac{1}{\rho}\sigma_n^2 \leq \gamma_i < P_{i,w}^r + \frac{1}{\rho}\sigma_n^2$. For $P_{i,w}^r + \frac{1}{\rho}\sigma_n^2 \leq \gamma_i < \rho\sigma_n^2$, we derive the first derivative with respect to γ_i as

$$T'(\gamma_i) = \frac{1}{2\ln(\rho)}\frac{P_{i,w}^r}{\gamma_i\left(\gamma_i - P_{i,w}^r\right)} > 0. \qquad (51)$$

For $\rho\sigma_n^2 \leq \gamma_i < \rho\sigma_n^2 + P_{i,w}^r$, we derive the first derivative with respect to γ_i as

$$T'(\gamma_i) = \frac{1}{2\ln(\rho)}\frac{1}{\rho\left(\gamma_i - P_{i,w}^r\right)} > 0. \qquad (52)$$

This demonstrates that $T(\gamma_i)$ is an increasing function of γ_i when $P_{i,w}^r + \frac{1}{\rho}\sigma_n^2 \leq \gamma_i < \rho\sigma_n^2$ and $\rho\sigma_n^2 \leq \gamma_i < \rho\sigma_n^2 + P_{i,w}^r$.

Although the derivative does not exist at $\gamma_i = P_{i,w}^r + \frac{1}{\rho}\sigma_n^2$ and $\gamma_i = \rho\sigma_n^2$, we can conclude that the minimum point of continuous function $T(\gamma_i)$ is located at $P_{i,w}^r + \frac{1}{\rho}\sigma_n^2$, which is also the optimal detection threshold $\gamma_i^* = P_{i,w}^r + \frac{1}{\rho}\sigma_n^2$ for the warden in BUM.

APPENDIX B
THE PROOF OF PROPOSITION 2 AND THEOREM 2

With UUM, substituting $\hat{f}_{\sigma_w^2}^{UUM}(\sigma_w^2)$ into (14), we can obtain the average error detection probability with respect to γ_i, which can be represented by a continuous piecewise function after some mathematical operations,

$$
T(\gamma_i) = \begin{cases} \frac{1}{2\mu_3} - \frac{1}{2\mu_3}\mathrm{erf}\left(\frac{\gamma_i - \mu_1}{\sqrt{2\mu_2}}\right), & \text{if } 0 < \gamma_i < P_{i,w}^r, \\ \frac{1}{2\mu_3}\left[1 + \mathrm{erf}\left(\frac{\gamma_i - P_{i,w}^r - \mu_1}{\sqrt{2\mu_2}}\right)\right. \\ \left. - \mathrm{erf}\left(\frac{-\mu_1}{\sqrt{2\mu_2}}\right) - \mathrm{erf}\left(\frac{\gamma_i - \mu_1}{\sqrt{2\mu_2}}\right)\right], & \text{otherwise.} \end{cases}
\tag{53}
$$

If $\frac{P_{i,w}^r}{2} + \mu_1 < P_{i,w}^r$, the first derivative with respect to γ_i is,

$$
T'(\gamma_i) = \begin{cases} \hat{T}_1(\gamma_i) < 0, & \text{if } 0 < \gamma_i < P_{i,w}^r, \\ \hat{T}_2(\gamma_i) > 0, & \text{otherwise.} \end{cases}
\tag{54}
$$

If $\frac{P_{i,w}^r}{2} + \mu_1 > P_{i,w}^r$, the first derivative with respect to γ_i is,

$$
T'(\gamma_i) = \begin{cases} \hat{T}_1(\gamma_i) < 0, & \text{if } 0 < \gamma_i < P_{i,w}^r, \\ \hat{T}_2(\gamma_i) < 0, & \text{if } P_{i,w}^r < \gamma_i < \mu_1 + \frac{P_{i,w}^r}{2}, \\ \hat{T}_2(\gamma_i) = 0, & \text{if } \gamma_i = \mu_1 + \frac{P_{i,w}^r}{2}, \\ \hat{T}_2(\gamma_i) > 0, & \text{otherwise.} \end{cases}
\tag{55}
$$

where

$$
\hat{T}_1(\gamma_i) = -\frac{1}{\sqrt{\pi}\mu_3}\exp\left(-\frac{(\gamma_i - \mu_1)^2}{2\mu_2}\right),
\tag{56}
$$

$$
\hat{T}_2(\gamma_i) = \frac{\exp\left(-\frac{(\gamma_i - P_{i,w}^r - \mu_1)^2}{2\mu_2}\right) - \exp\left(-\frac{(\gamma_i - \mu_1)^2}{2\mu_2}\right)}{\sqrt{2\pi\mu_2}\mu_3}.
\tag{57}
$$

To sum up, the optimal threshold for the warden is $\gamma_i^* = \max\left\{P_{i,w}^r, \frac{P_{i,w}^r}{2} + \mu_1\right\}$, which is consistent with that of [28].

Substituting γ_i^* into (13) and considering the detailed expressions of μ_1, μ_2, and μ_3, we have

$$
\begin{aligned}
\bar{\delta}_i &= \int_0^\infty \delta_i(\sigma_w^2, \gamma_i^*)\hat{f}_{\sigma_w^2}^{UUM}(\sigma_w^2)\mathrm{d}\sigma_w^2 \\
&= \begin{cases} 1 - \frac{1}{\mu_3}\mathrm{erf}\left(\frac{P_{i,w}^r}{2\sqrt{2\mu_2}}\right), & \text{if } P_{i,w}^r < 2\mu_1, \\ \frac{1}{2\mu_3}\left(1 - \mathrm{erf}\left(\frac{P_{i,w}^r - \mu_1}{\sqrt{2\mu_2}}\right)\right), & \text{otherwise.} \end{cases}
\end{aligned}
\tag{58}
$$

With $\bar{\delta}_i \geq 1 - \epsilon$, the maximum received power $P_{i,w}^r$ satisfies

$$
P_{i,w}^r = \begin{cases} 2\sqrt{2\mu_2}\mathrm{erf}^{-1}(\epsilon\mu_3), & \text{if } \epsilon < \frac{\mu_4}{\mu_3}, \\ \mu_1 + \sqrt{2\mu_2}\mathrm{erf}^{-1}\left(2\mu_3\epsilon - \mu_4\right), & \text{otherwise.} \end{cases}
\tag{59}
$$

Thus, the maximum RII provided by anchor $\boldsymbol{a}_i$ is

$$
\lambda_i = \begin{cases} 2\sqrt{2\mu_2}\left(\frac{d_{i,w}}{d_{i,b}}\right)^\varrho \frac{\xi_i}{A^o}\mathrm{erf}^{-1}(\epsilon\mu_3), & \text{if } \epsilon < \frac{\mu_4}{\mu_3}, \\ \mu_1\left(\frac{d_{i,w}}{d_{i,b}}\right)^\varrho \frac{\xi_i}{A^o} \\ + \left(\frac{d_{i,w}}{d_{i,b}}\right)^\varrho \frac{\xi_i}{A^o}\sqrt{2\mu_2}\mathrm{erf}^{-1}\left(2\mu_3\epsilon - \mu_4\right), & \text{otherwise,} \end{cases}
\tag{60}
$$

and CSPEB can be calculated by substituting $\lambda_i, \forall i \in \mathcal{N}_a$ into (18) and (19).

APPENDIX C
THE PROOF OF REMARK 2

From the expression of $P_C^{UUM}(\boldsymbol{b})$, ϵ, $\sigma_{n,\mathrm{dB}}^2$, and $\sigma_{\Delta,\mathrm{dB}}^2$ are independent with $\sum_{i=1}^N \left(\frac{d_{i,w}}{d_{i,b}}\right)^\varrho \xi_i \boldsymbol{J}_r(\phi_i)$. Thus, we only focus on the effect of ϵ and $\sigma_{\Delta,\mathrm{dB}}^2$ on the rest of CSPEB. As known, the first derivative of inverse error function $\mathrm{erf}^{-1}(\cdot)$ is positive due to the fact that inverse error function $\mathrm{erf}^{-1}(\cdot)$ has the same monotonicity as the error function $\mathrm{erf}(\cdot)$.

A. $P_C^{UUM}(\boldsymbol{b})$ With Respect to ϵ

In the first part of the piecewise function, i.e., $\epsilon < \frac{\mu_4}{\mu_3}$, the first derivative of $2\sqrt{2\mu_2}\mathrm{erf}^{-1}(\epsilon\mu_3)$ with respect to ϵ is

$$
\frac{\partial}{\partial\epsilon}2\sqrt{2\mu_2}\mathrm{erf}^{-1}(\epsilon\mu_3) = 2\sqrt{2\mu_2}\mu_3 B_1 > 0,
\tag{61}
$$

where $B_1 = \left.\frac{\partial}{\partial x}\mathrm{erf}^{-1}(x)\right|_{x=\epsilon\mu_3} > 0$. If $\frac{\mu_4}{\mu_3} < \epsilon < 1$, the first derivative of $\mu_1 + \sqrt{2\mu_2}\mathrm{erf}^{-1}\left(2\mu_3\epsilon - \mu_4\right)$ with respect to ϵ is

$$
\frac{\partial}{\partial\epsilon}\left(\mu_1 + \sqrt{2\mu_2}\mathrm{erf}^{-1}\left(2\mu_3\epsilon - \mu_4\right)\right) = 2B_2\sqrt{2\mu_2}\mu_3 > 0,
\tag{62}
$$

where $B_2 = \left.\frac{\partial}{\partial x}\mathrm{erf}^{-1}(x)\right|_{x=2\mu_3\epsilon - \mu_4} > 0$. Thus, $2\sqrt{2\mu_2}\mathrm{erf}^{-1}(\epsilon\mu_3)$ monotonically increases with respect to ϵ, and is not equal to 0 due to $\epsilon\mu_3 > 0$. Therefore, the continuous piecewise function $P_C^{UUM}(\boldsymbol{b})$ decreases with the covertness requirement coefficient ϵ.

B. $P_C^{UUM}(\boldsymbol{b})$ With Respect to $\sigma_{\Delta,\mathrm{dB}}^2$

The first derivatives of μ_1, μ_2, and μ_3 with respect to $\sigma_{\Delta,\mathrm{dB}}^2$ are given by

$$
\frac{\partial\mu_1}{\partial\sigma_{\Delta,\mathrm{dB}}^2} = \frac{k^2}{2}\mu_1, \quad \frac{\partial\mu_2}{\partial\sigma_{\Delta,\mathrm{dB}}^2} = k^2\mu_1^2 + 2k^2\mu_2,
$$

$$
\frac{\partial\mu_3}{\partial\sigma_{\Delta,\mathrm{dB}}^2} = k^2\frac{\mu_1^3 + \mu_1\mu_2}{2\sqrt{2\pi\mu_2}\mu_2}\exp\left(-\left(\frac{\mu_1}{\sqrt{2\mu_2}}\right)^2\right).
\tag{63}
$$

If $\epsilon < \frac{1}{\mu_3}\mathrm{erf}\left(\frac{\mu_1}{\sqrt{2\mu_2}}\right)$, the first derivative of $2\sqrt{2\mu_2}\mathrm{erf}^{-1}(\epsilon\mu_3)$ with respect to $\sigma_{\Delta,\mathrm{dB}}^2$ is

$$
\begin{aligned}
&\frac{\partial}{\partial\sigma_{\Delta,\mathrm{dB}}^2}(2\sqrt{2\mu_2}\mathrm{erf}^{-1}(\epsilon\mu_3)) \\
&= \frac{4B_1\mu_2 + \left(2k^2\mu_1^2 + 4k^2\mu_2\right)\mathrm{erf}^{-1}(\epsilon\mu_3)}{\sqrt{2\mu_2}} > 0.
\end{aligned}
\tag{64}
$$

Otherwise, if $\frac{\mu_4}{\mu_3} < \epsilon < 1$, the first derivative of $\mu_1 + \sqrt{2\mu_2}\text{erf}^{-1}(2\mu_3\epsilon - \mu_4)$ with respect to $\sigma_{\Delta,\text{dB}}^2$ is

$$\frac{\partial}{\partial \sigma_{\Delta,\text{dB}}^2}\left(\mu_1 + \sqrt{2\mu_2}\text{erf}^{-1}(2\mu_3\epsilon - \mu_4)\right)$$
$$= \frac{k^2}{2}\mu_1 + \sqrt{2\mu_2}B_2 + \frac{k^2\mu_1^2 + 2k^2\mu_2}{\sqrt{2\mu_2}}B_3 > 0, \quad (65)$$

where $B_3 = \text{erf}^{-1}(2\mu_3\epsilon - \mu_4)$. It is obvious that $B_3 > 0$, due to the fact that $\mu_3\epsilon > \mu_4$. Thus, $\mu_1 + \sqrt{2\mu_2}\text{erf}^{-1}(2\mu_3\epsilon - \mu_4)$ monotonically increases with respect to $\sigma_{\Delta,\text{dB}}^2$, for any ϵ. Therefore, the continuous piecewise function $P_C^{UUM}(\boldsymbol{b})$ monotonically decreases with respect to noise uncertainty coefficient $\sigma_{\Delta,\text{dB}}^2$.

C. $P_C^{UUM}(\boldsymbol{b})$ With Respect to $\sigma_{n,\text{dB}}^2$

We have the first derivatives of μ_1, μ_2, and μ_3 with respect to $\sigma_{n,\text{dB}}^2$,

$$\frac{\partial \mu_1}{\partial \sigma_{n,\text{dB}}^2} = k\mu_1, \quad \frac{\partial \mu_2}{\partial \sigma_{n,\text{dB}}^2} = 2k\mu_2, \quad \frac{\partial \mu_3}{\partial \sigma_{n,\text{dB}}^2} = 0. \quad (66)$$

If $\epsilon < \frac{\mu_4}{\mu_3}$, the first derivative of $2\sqrt{2\mu_2}\text{erf}^{-1}(\epsilon\mu_3)$ with respect to $\sigma_{n,\text{dB}}^2$ is

$$\frac{\partial(2\sqrt{2\mu_2}\text{erf}^{-1}(\epsilon\mu_3))}{\partial \sigma_{n,\text{dB}}^2} = 2k\sqrt{2\mu_2}\text{erf}^{-1}(\epsilon\mu_3) > 0, \quad (67)$$

Otherwise, if $\frac{\mu_4}{\mu_3} < \epsilon < 1$, the first derivative of $\mu_1 + \sqrt{2\mu_2}\text{erf}^{-1}(2\mu_3\epsilon - \mu_4)$ with respect to $\sigma_{n,\text{dB}}^2$ is

$$\frac{\partial}{\partial \sigma_{n,\text{dB}}^2}\left(\mu_1 + \sqrt{2\mu_2}\text{erf}^{-1}(2\mu_3\epsilon - \mu_4)\right)$$
$$= k\left(\mu_1 + \sqrt{2\mu_2}\text{erf}^{-1}(2\mu_3\epsilon - \mu_4)\right) > 0. \quad (68)$$

Thus, $P_C^{UUM}(\boldsymbol{b})$ monotonically decreases with respect to the nominal noise power $\sigma_{n,\text{dB}}^2$.

REFERENCES

[1] F. Lyu et al., "Characterizing urban Vehicle-to-Vehicle communications for reliable safety applications," *IEEE Trans. Intell. Transp. Syst.*, vol. 21, no. 6, pp. 2586–2602, Jun. 2020.

[2] M. Z. Win, W. Dai, Y. Shen, G. Chrisikos, and H. Vincent Poor, "Network operation strategies for efficient localization and navigation," *Proc. IEEE*, vol. 106, no. 7, pp. 1224–1254, Jul. 2018.

[3] S. He, D.-H. Shin, J. Zhang, and J. Chen, "Near-optimal allocation algorithms for location-dependent tasks in crowdsensing," *IEEE Trans. Veh. Technol.*, vol. 66, no. 4, pp. 3392–3405, Apr. 2017.

[4] N. Cheng et al., "Big data driven vehicular networks," *IEEE Netw.*, vol. 32, no. 6, pp. 160–167, Nov. 2018.

[5] P. Yang, N. Zhang, S. Zhang, L. Yu, J. Zhang, and X. Shen, "Content popularity prediction towards location-aware mobile edge caching," *IEEE Trans. Multimedia*, vol. 21, no. 4, pp. 915–929, Apr. 2019.

[6] Y. Zhao, Z. Li, B. Hao, and J. Shi, "Sensor selection for TDOA-based localization in wireless sensor networks with Non-Line-of-Sight condition," *IEEE Trans. Veh. Technol.*, vol. 68, no. 10, pp. 9935–9950, Oct. 2019.

[7] S. Amuru, H. S. Dhillon, and R. M. Buehrer, "On jamming against wireless networks," *IEEE Trans. Wireless Commun.*, vol. 16, no. 1, pp. 412–428, Jan. 2017.

[8] J. H. Lee and R. M. Buehrer, "Characterization and detection of location spoofing attacks," *J. Commun. Netw.*, vol. 14, no. 4, pp. 396–409, Aug. 2012.

[9] L. Cong and W. Zhuang, "Hybrid TDOA/AOA mobile user location for wideband CDMA cellular systems," *IEEE Trans. Wireless Commun.*, vol. 1, no. 3, pp. 439–447, Jul. 2002.

[10] K. Zheng et al., "Energy-efficient localization and tracking of mobile devices in wireless sensor networks," *IEEE Trans. Veh. Technol.*, vol. 66, no. 3, pp. 2714–2726, Mar. 2017.

[11] H. Li, Y. He, X. Cheng, H. Zhu, and L. Sun, "Security and privacy in localization for underwater sensor networks," *IEEE Commun. Mag.*, vol. 53, no. 11, pp. 56–62, Nov. 2015.

[12] K. Mehta, D. Liu, and M. Wright, "Location privacy in sensor networks against a global eavesdropper," in *Proc. IEEE Int. Conf. Netw. Protocols*, Oct. 2007, pp. 314–323.

[13] T. Zhang, X. Li, and Q. Zhang, "Location privacy protection: A power allocation approach," *IEEE Trans. Commun.*, vol. 67, no. 1, pp. 748–761, Jan. 2019.

[14] T. Wang and Y. Yang, "Analysis on perfect location spoofing attacks using beamforming," in *Proc. IEEE INFOCOM*, Apr. 2013, pp. 2778–2786.

[15] R. Zekavat and R. M. Buehrer, *Handbook of Position Location: Theory, Practice and Advances*, vol. 27. Hoboken, NJ, USA: Wiley, 2011.

[16] S. Capkun and J.-P. Hubaux, "Secure positioning in wireless networks," *IEEE J. Sel. Areas Commun.*, vol. 24, no. 2, pp. 221–232, Feb. 2006.

[17] D. Liu, P. Ning, and W. Kevin Du, "Attack-resistant location estimation in sensor networks," in *Proc. 4th Int. Symp. Inf. Process. Sensor Netw.*, Apr. 2005, pp. 99–106.

[18] J. Zhang, X. Wang, R. S. Blum, and L. M. Kaplan, "Attack detection in sensor network target localization systems with quantized data," *IEEE Trans. Signal Process.*, vol. 66, no. 8, pp. 2070–2085, Apr. 2018.

[19] K. Lim, K. M. Tuladhar, and H. Kim, "Detecting location spoofing using ADAS sensors in VANETs," in *Proc. 16th IEEE Annu. Consum. Commun. Netw. Conf. (CCNC)*, Jan. 2019, pp. 1–4.

[20] D. Liu, P. Ning, and W. Du, "Detecting malicious beacon nodes for secure location discovery in wireless sensor networks," in *Proc. 25th IEEE Int. Conf. Distrib. Comput. Syst. (ICDCS)*, Jun. 2005, pp. 609–619.

[21] A. Boukerche, H. A. B. Oliveira, E. F. Nakamura, and A. A. F. Loureiro, "Secure localization algorithms for wireless sensor networks," *IEEE Commun. Mag.*, vol. 46, no. 4, pp. 96–101, Apr. 2008.

[22] Z. Li, W. Trappe, Y. Zhang, and B. Nath, "Robust statistical methods for securing wireless localization in sensor networks," in *Proc. 4th Int. Symp. Inf. Process. Sensor Netw.*, Apr. 2005, pp. 91–98.

[23] L. Lazos and R. Poovendran, "HiRLoc: High-resolution robust localization for wireless sensor networks," *IEEE J. Sel. Areas Commun.*, vol. 24, no. 2, pp. 233–246, Feb. 2006.

[24] K. Shahzad, X. Zhou, and S. Yan, "Covert communication in fading channels under channel uncertainty," in *Proc. IEEE 85th Veh. Technol. Conf.*, Jun. 2017, pp. 1–5.

[25] B. He, S. Yan, X. Zhou, and H. Jafarkhani, "Covert wireless communication with a Poisson field of interferers," *IEEE Trans. Wireless Commun.*, vol. 17, no. 9, pp. 6005–6017, Sep. 2018.

[26] Z. Liu, J. Liu, Y. Zeng, and J. Ma, "Covert wireless communications in IoT systems: Hiding information in interference," *IEEE Wireless Commun.*, vol. 25, no. 6, pp. 46–52, Dec. 2018.

[27] S. Lee, R. J. Baxley, M. A. Weitnauer, and B. Walkenhorst, "Achieving undetectable communication," *IEEE J. Sel. Topics Signal Process.*, vol. 9, no. 7, pp. 1195–1205, Oct. 2015.

[28] B. He, S. Yan, X. Zhou, and V. K. N. Lau, "On covert communication with noise uncertainty," *IEEE Commun. Lett.*, vol. 21, no. 4, pp. 941–944, Apr. 2017.

[29] J. Hu, S. Yan, X. Zhou, F. Shu, J. Li, and J. Wang, "Covert communication achieved by a greedy relay in wireless networks," *IEEE Trans. Wireless Commun.*, vol. 17, no. 7, pp. 4766–4779, Jul. 2018.

[30] K. Shahzad, X. Zhou, S. Yan, J. Hu, F. Shu, and J. Li, "Achieving covert wireless communications using a full-duplex receiver," *IEEE Trans. Wireless Commun.*, vol. 17, no. 12, pp. 8517–8530, Dec. 2018.

[31] T. V. Sobers, B. A. Bash, S. Guha, D. Towsley, and D. Goeckel, "Covert communication in the presence of an uninformed jammer," *IEEE Trans. Wireless Commun.*, vol. 16, no. 9, pp. 6193–6206, Sep. 2017.

[32] Z. Li, L. Guan, C. Li, and A. Radwan, "A secure intelligent spectrum control strategy for future THz mobile heterogeneous networks," *IEEE Commun. Mag.*, vol. 56, no. 6, pp. 116–123, Jun. 2018.

[33] R. Tandra and A. Sahai, "SNR walls for signal detection," *IEEE J. Sel. Topics Signal Process.*, vol. 2, no. 1, pp. 4–17, Feb. 2008.

[34] E. Axell, G. Leus, E. Larsson, and H. Poor, "Spectrum sensing for cognitive radio : State-of-the-Art and recent advances," *IEEE Signal Process. Mag.*, vol. 29, no. 3, pp. 101–116, May 2012.

[35] A. Sonnenschein and P. M. Fishman, "Radiometric detection of spread-spectrum signals in noise of uncertain power," *IEEE Trans. Aerosp. Electron. Syst.*, vol. 28, no. 3, pp. 654–660, Jul. 1992.

[36] Y. Shen and M. Z. Win, "Fundamental limits of wideband Localization—Part I: A general framework," *IEEE Trans. Inf. Theory*, vol. 56, no. 10, pp. 4956–4980, Oct. 2010.

[37] D. Wang, N. Zhang, Z. Li, F. Gao, and X. Shen, "Leveraging high order cumulants for spectrum sensing and power recognition in cognitive radio networks," *IEEE Trans. Wireless Commun.*, vol. 17, no. 2, pp. 1298–1310, Feb. 2018.

[38] T. Zhang, A. F. Molisch, Y. Shen, Q. Zhang, H. Feng, and M. Z. Win, "Joint power and bandwidth allocation in wireless cooperative localization networks," *IEEE Trans. Wireless Commun.*, vol. 15, no. 10, pp. 6527–6540, Oct. 2016.

[39] T. Zhang, C. Qin, A. F. Molisch, and Q. Zhang, "Joint allocation of spectral and power resources for non-cooperative wireless localization networks," *IEEE Trans. Commun.*, vol. 64, no. 9, pp. 3733–3745, Sep. 2016.

[40] Z. Li *et al.*, "Multiobjective optimization based sensor selection for TDOA tracking in wireless sensor network," *IEEE Trans. Veh. Technol.*, vol. 68, no. 12, pp. 12360–12374, Dec. 2019.

Wei Wang (Member, IEEE) received the B.Eng. degree in information countermeasure technology and the M.Eng. degree in signal and information processing from Xidian University, Xi'an, China, in 2011 and 2014, respectively, and the Ph.D. degree in electrical and electronic engineering from Nanyang Technological University, Singapore, in 2018. He was as a Post-Doctoral Fellow with the Department of Electrical and Computer Engineering, University of Waterloo, Waterloo, ON, Canada, from September 2018 to September 2019. He is currently a Professor with the College of Electronic and Information Engineering, Nanjing University of Aeronautics and Astronautics, Nanjing, China. His research interests include wireless communications, space-air-ground integrated networks, wireless security, and electromagnetic spectrum security. He was a recipient of the IEEE Student Travel Grants for IEEE ICC'17 and the Chinese Government Award for outstanding self-financed students abroad in 2018.

Yue Zhao (Graduate Student Member, IEEE) received the B.S. degree from the College of Information Science and Engineering, Shanxi Agricultural University, Jinzhong, China, in 2015, and the Ph.D. degree from the School of Telecommunications Engineering, Xidian University, Xi'an, China, in 2020. From November 2018 to October 2019, he was a Visiting Student with the Broadband Communications Research (BBCR) Group, Department of Electrical and Computer Engineering, University of Waterloo, Waterloo, ON, Canada. He is currently an Associate Professor with the State Key Laboratory of ISN, School of Telecommunication Engineering, Xidian University. His research interests include wireless network localization, covert communications, and space-air-ground integrated networks.

Chenxi Li (Graduate Student Member, IEEE) received the B.S. degree in communication engineering from Zhengzhou University, Zhengzhou, China, in 2015. She is currently pursuing the Ph.D. degree in military communications with the State Key Laboratory of ISN, School of Telecommunication Engineering, Xidian University, Xi'an, China. Since May 2020, she has been a Visiting Student with the Broadband Communications Research (BBCR) Group, Department of Electrical and Computer Engineering, University of Waterloo, Waterloo, ON, Canada. Her research interests include wireless communications and networks, with current emphasis on the intelligent spectrum control and covert communication.

Zan Li (Senior Member, IEEE) received the B.S. degree in communications engineering and the M.S. and Ph.D. degrees in communication and information systems from Xidian University, Xi'an, China, in 1998, 2001, and 2006, respectively. She is currently a Professor with the State Key Laboratory of ISN, School of Telecommunication Engineering, Xidian University. Her research interests include wireless communication and signal processing, particularly covert communication, weak signal detection, spectrum sensing, and cooperative communication. She is a fellow of the Institution of Engineering and Technology (IET), the China Institute of Electronics (CIE), and the China Institute of Communications (CIC). She serves as an Associate Editor for the IEEE TRANSACTIONS ON COGNITIVE COMMUNICATIONS AND NETWORKING and *China Communications*.

Xuemin (Sherman) Shen (Fellow, IEEE) received the Ph.D. degree in electrical engineering from Rutgers University, New Brunswick, NJ, USA, in 1990. He is currently a University Professor with the Department of Electrical and Computer Engineering, University of Waterloo, Waterloo, ON, Canada. His research interests include resource management in interconnected wireless/wired networks, wireless network security, social networks, smart grid, and vehicular ad-hoc and sensor networks. He is a Registered Professional Engineer of Ontario, Canada, an Engineering Institute of Canada Fellow, a Canadian Academy of Engineering Fellow, a Royal Society of Canada Fellow, and a Distinguished Lecturer of the IEEE Vehicular Technology Society and the Communications Society.

He received the R.A. Fessenden Award in 2019 from the IEEE, Canada, the James Evans Avant Garde Award in 2018 from the IEEE Vehicular Technology Society, the Joseph LoCicero Award in 2015, and the Education Award in 2017 from the IEEE Communications Society. He has also received the Excellent Graduate Supervision Award in 2006 and the Outstanding Performance Award five times from the University of Waterloo and the Premier's Research Excellence Award (PREA) in 2003 from the Province of Ontario, Canada. He served as the Technical Program Committee Chair/Co-Chair for the IEEE Globecom'16, the IEEE Infocom'14, the IEEE VTC'10 Fall, and the IEEE Globecom'07, the Symposia Chair for the IEEE ICC'10, the Tutorial Chair for the IEEE VTC'11 Spring, and the Chair for the IEEE Communications Society Technical Committee on Wireless Communications and the P2P Communications and Networking. He is the Vice President of Publications of the IEEE Communications Society.

Nan Cheng (Member, IEEE) received the B.E. and M.S. degrees from the Department of Electronics and Information Engineering, Tongji University, Shanghai, China, in 2009 and 2012, respectively, and the Ph.D. degree from the Department of Electrical and Computer Engineering, University of Waterloo, in 2016. He was a Post-Doctoral Fellow with the Department of Electrical and Computer Engineering, University of Toronto, from 2017 to 2018. He is currently a Professor with the State Key Laboratory of ISN, School of Telecommunication Engineering, Xidian University, Xi'an, China. His current research interests include space-air-ground integrated systems, big data in vehicular networks, self-driving systems, performance analysis, MAC, opportunistic communication, and application of AI for vehicular networks.